

Novel Bis(1*H*-indol-2-yl)methanones as Potent Inhibitors of FLT3 and Platelet-Derived Growth Factor Receptor Tyrosine Kinase

Siavosh Mahboobi,^{†,§,*} Andrea Uecker,^{‡,§} Andreas Sellmer,[†] Christophe Cénac,[†] Heymo Höcher,[†] Herwig Pongratz,[†] Emerich Eichhorn,[†] Harald Hufsky,^{†,⊗} Antje Trümpler,[‡] Marit Sicker,[‡] Florian Heidel,^{||} Thomas Fischer,^{||} Carol Stocking,[⊥] Sigurd Elz,[†] Frank-D. Böhmer,^{‡,§,*} and Stefan Dove^{†,§}

Institute of Pharmacy, Faculty of Chemistry and Pharmacy, University of Regensburg, D-93040 Regensburg, Germany; Institute of Molecular Cell Biology, Jena University Hospital, D-07747 Jena, Germany; Department of Medicine III, Hematology-Oncology, University of Mainz, D-55101 Mainz, Germany; and Research Group Molecular Pathology, Heinrich-Pette-Institute, D-20251, Hamburg, Germany

Received June 14, 2005

FLT3 receptor tyrosine kinase is aberrantly active in many cases of acute myeloid leukemia (AML). Recently, bis(1*H*-indol-2-yl)methanones were found to inhibit FLT3 and PDGFR kinases. To optimize FLT3 activity and selectivity, 35 novel derivatives were synthesized and tested for inhibition of FLT3 and PDGFR autophosphorylation. The most potent FLT3 inhibitors **98** and **102** show IC₅₀ values of 0.06 and 0.04 μM, respectively, and 1 order of magnitude lower PDGFR inhibiting activity. The derivatives **76** and **82** are 20- to 40-fold PDGFR selective. Docking at the recent FLT3 structure suggests a bidentate binding mode with the backbone of Cys-694. Activity and selectivity can be related to interactions of one indole moiety with a hydrophobic pocket including Phe-691, the only different binding site residue (PDGFR Thr-681). Compound **102** inhibited the proliferation of 32D cells expressing wildtype FLT3 or FLT3-ITD similarly as FLT3 autophosphorylation, and induced apoptosis in primary AML patient blasts.

Introduction

One of the hallmarks in cancer development is the acquisition of growth factor independence.¹ Aberrant activation of tyrosine kinases often represents the underlying mechanism.² Both, activated cytoplasmic or receptor tyrosine kinases can drive growth factor-independent proliferation and, therefore, represent suitable targets for cancer therapy. Since molecular defects in tyrosine kinases usually represent only one of multiple molecular lesions in a given cancer cell, the beneficial effects of tyrosine kinase inhibition may be very variable. Definition of patient populations which will maximally benefit from tyrosine kinase inhibition, use of selective inhibitors of mutated kinase versions or of drugs which inhibit a panel of targets in a “multitargeted” fashion, and combination with other types of therapy, are issues which are currently intensely pursued.^{3–5} Survival and subsequent propagation of resistant molecular versions of tyrosine kinases under chronic medication is another recently observed phenomenon, often resulting in relapse of the tumor.⁶ Obviously, there is a need for compounds with novel therapeutic profiles based on specific binding modes, well-defined kinase selectivity and activity toward clinically relevant kinase mutants.

Fms-like (McDonough feline sarcoma viral oncogene homologue-like) tyrosine kinase 3 (FLT3) is aberrantly active in many cases of acute myeloid leukemia (AML).⁷ Mutations conferring constitutive kinase activity are found in up to 30% of cases. Most prevalent are mutations denoted “internal tandem duplications” (ITD) which occur in the juxtamembrane domain of the

kinase. Activating point mutations in the kinase activation loop are found in another subset of patients. Finally, elevated expression of wildtype FLT3 and autocrine activation by its cognate ligand FL (FLT3 ligand) is found in many other cases of AML and may potentially also contribute to the disease.⁸ Compounds of several structural families, including quinoxalines such as **1a** (AG1295) and **1b** (AGL2043), the indolinones **1c** (SU5416) and **1d** (SU11248), the indolocarbazoles **1e** (PKC412, Midostaurin) and **1f** (CEP701), and the piperazonylquinazoline **1g** (CT53518) are potent inhibitors of FLT3 kinase (lit.⁷ and references therein), as well as the quinoline-urea Ki23819 (exact structure and chemical name not published yet⁹). Some of them have been promising in first clinical trials. FLT3 is, however, refractory for inhibition by **2** (STI571, Imatinib, Glivec, Gleevec),¹⁰ the potent inhibitor of Abl/Bcr-Abl, c-Kit, and PDGFR. Phe691 in the ATP binding site of FLT3 prevents binding of **2**.¹¹

We have previously reported the inhibition of the class III receptor tyrosine kinase PDGFR by the bis(1*H*-indol-2-yl)-methanone **3** and more particularly by its monosubstituted derivatives, as for example those depicted in Figure 1 (see also Table 1 and lit.¹²). Members of this compound family, like **4a** (known as D-64406), are also reasonably potent inhibitors of FLT3 (cf. Table 1 and lit.¹³). However, the 5-monosubstituted derivatives investigated so far were rather PDGFR-selective or at the most equiactive at both kinases. The question arose whether FLT3 selectivity may be obtained by variation of other positions or even more by substitution of both indole moieties. This strategy appeared reasonable since the previous data and models indicated that the unsubstituted indole fits to the internal walls of the binding pockets containing the only significant differences of FLT3 and PDGFR. Here, we present synthesis and structure–activity relationships (SAR) for novel, more potent FLT3 inhibitors of the bisindolylmethanone family. Despite the close similarity of the inhibitor binding pockets, some compounds exhibit selectivity for FLT3 versus PDGFR

* General correspondence and correspondence on chemical aspects to Siavosh Mahboobi [e-mail: siavosh.mahboobi@chemie.uni-regensburg.de, fax: +49 (0)941 943 1737, phone: +49 (0)941 943 4824]. Correspondence on biological aspects to Frank-D. Böhmer [e-mail: i5frbo@rz.uni-jena.de].

[†] University of Regensburg.

[‡] Jena University Hospital.

^{||} University of Mainz.

[⊥] Heinrich-Pette-Institute.

[⊗] Present address: Novartis Pharma AG, CH-4057 Basel, Switzerland.

[§] Authors contributed equally to this work.

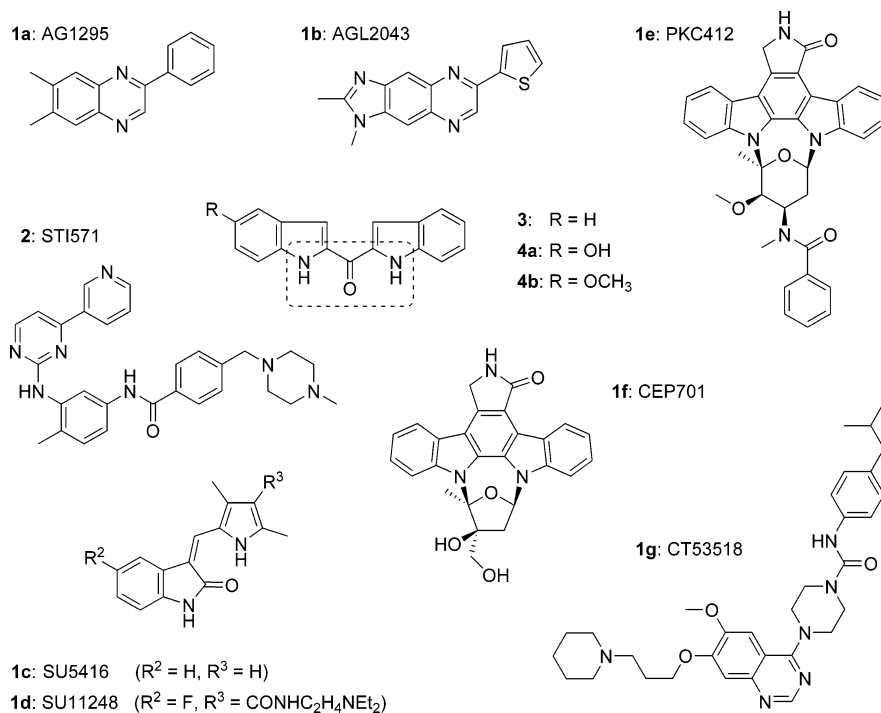
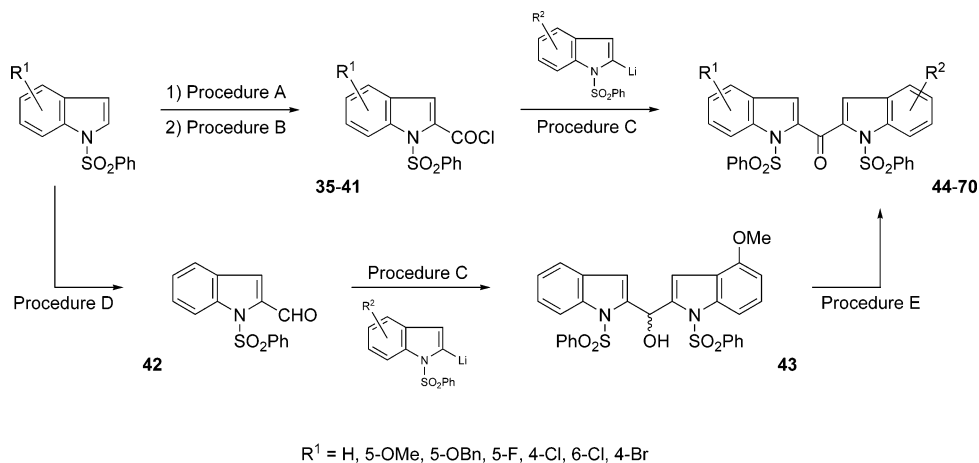


Figure 1. Bisindolylmethanone (**3**) and selected monosubstituted derivatives (**4a** and **4b**) as leads for the development of novel FLT3 inhibitors, along with structures of known FLT3 and PDGFR inhibitors.

Scheme 1^a



^a A: (1) *n*-BuLi or LDA, THF, -78 °C; (2) CO₂ (s). B: SOCl₂, reflux. C: THF, -78 °C. D: (1) *n*-BuLi or LDA, THF, -78 °C; (2) DMF. E: PDC/PTFA, DCM, 25 °C.

and vice versa. The structure–activity and -selectivity relationships are explained with the help of molecular models of inhibitor–kinase complexes based on the novel PDB crystal structure 1rjb of FLT3.¹⁴

Chemistry

Since the 1,3-di(*sec*-amino)propan-2-one substructure (emphasized in Figure 1) seemed to be essential for kinase inhibition,¹² the bis(1*H*-indol-2-yl)methanone scaffold was retained unchanged throughout the series, aside from two compounds synthesized in order to verify the suggested binding mode at FLT3. According to the previous SAR of PDGFR inhibition,¹² one indole moiety was substituted in 5-position mostly by hydroxy or methoxy groups. Assuming that the interior of the binding site is spatially restricted, substituents of the second indole should be rather small, but cover a certain range of hydrophobic and electronic properties. Therefore

especially halogens, methyl, and hydroxy/alkoxy groups were introduced in different positions.

The *N*-phenylsulfonylated bisindolylmethanones **45–68** were synthesized according to Scheme 1 by coupling of an indolyl carboxylic acid chloride (**35–38**, **40**) with its respective lithiated indolyl. The acyl chlorides **35–41** themselves were obtained from their corresponding *N*-protected indoles (**6**, **11**, **14**, **16**, **19**, **21**, and **23**) following Procedures A and B (see legend of Scheme 1). Furthermore the desired bis(1-phenylsulfonyl-1*H*-indol-2-yl)methanones (**44**) can be prepared by coupling of the respective aldehydes (**42**) and 2-lithiated indoles, followed by oxidation of the resulting carbinols (**43**).

Deprotection of the *N*-phenylsulfonylated ketones **44–68** by tetra-*n*-butylammonium fluoride or sodium hydroxide led to the respective bis(1*H*-indol-2-yl)methanone derivatives **72–96** (Scheme 2). The (5-benzyloxy-1*H*-indol-2-yl)(7-ethyl-1*H*-indol-2-yl)methanone **97** was obtained by modification of the usual

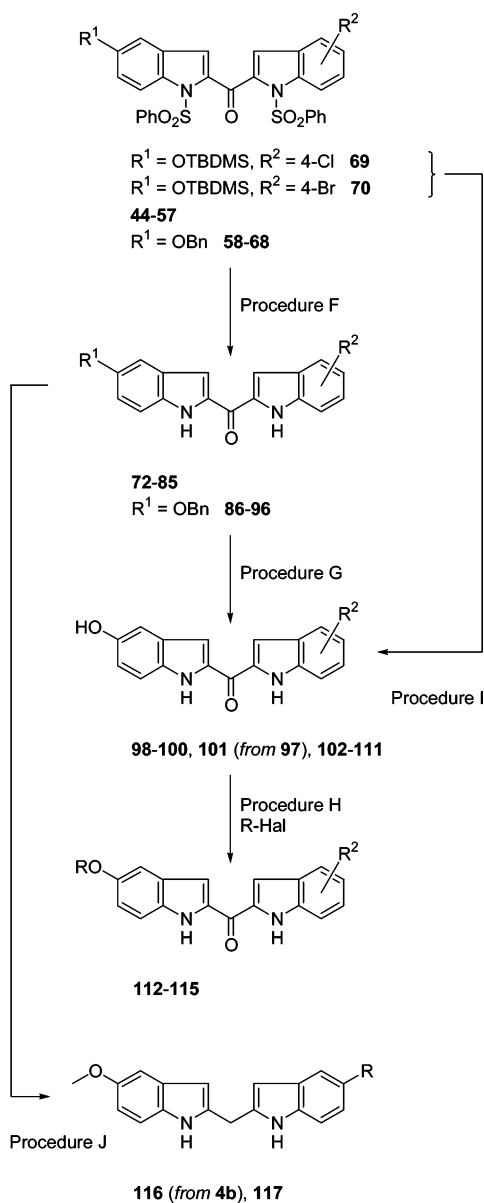
Table 1. Inhibition of FLT3 and PDGFR Tyrosine Kinases by Bis(1*H*-indol-2-yl)methanones and Related Compounds in Cell Assays

Cpd.	Substituent R ¹	Substituent R ²	FLT3 ^(a) IC ₅₀ (μM)	PDGFR ^(b) IC ₅₀ (μM)
3 ^(c)	H	H	4.6	1
4a ^(c)	OH	H	0.57	0.2
4b ^(c)	OCH ₃	H	3.2	0.3 [#]
4c ^(c)	OCH ₂ Ph	H	10 - 30	10 - 30
5 ^(c)	H	6'-OCH ₃	0.89	0.3
72	H	4'-OCH ₃	4.4	1.5
73	F	H	2.3	0.76
74	OCH ₃	4'-CH ₃	2.6	4.03
75	OCH ₃	5'-CH ₃	10 - 30	> 30
76	OCH ₃	6'-CH ₃	10 - 30	0.51 [#]
77	OCH ₃	4'-F	10 - 30	8.1
78	OCH ₃	5'-F	0.88	0.4
79	OCH ₃	6'-F	7.6	0.84 [#]
80	OCH ₃	4'-Cl	10 - 30	> 30
81	OCH ₃	5'-Cl	11.0	2.5
82	OCH ₃	6'-Cl	9.4	0.20 [#]
83	OCH ₃	7'-Cl	> 30	> 30
84	OCH ₃	5'-Br	9.9	8.5
85	F	4'-CH ₃	2.6	1.2
91	OCH ₂ Ph	6'-OCH ₃	10 - 30	> 30
94	OCH ₂ Ph	5'-F	> 30	5.8
98	OH	4'-CH ₃	0.06 [#]	0.96
99	OH	5'-CH ₃	0.74	3.5
100	OH	6'-CH ₃	1.2	0.58
101	OH	7'-CH ₂ CH ₃	10 - 30	4.4
102	OH	5'-OH	0.04 [#]	0.3
103	OH	4'-OCH ₃	0.67	0.96
104	OH	6'-OCH ₃	0.53	0.65
105	OH	7'-OCH ₃	6.6	2.9
106	OH	4'-F	0.34	0.62
107	OH	5'-F	0.17	0.73
108	OH	6'-F	1	0.59
109	OH	7'-F	> 30	4.8
110	OH	4'-Cl	0.92	0.5
111	OH	4'-Br	3.4	6.1
112	O(CH ₂) ₂ NMe ₂	6'-OCH ₃	6.7	2.8
113	2-piperidin-1-ylethoxy	4'-CH ₃	0.70 [#]	10 - 30
114	2-piperidin-1-ylethoxy	6'-OCH ₃	1.3	1.0
115	2-piperidin-1-ylethoxy	5'-F	1.5	0.50

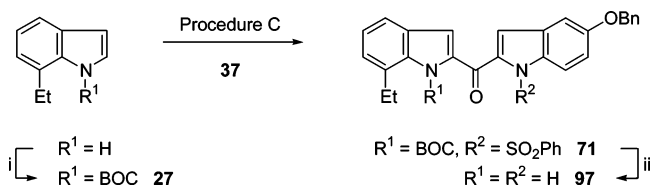
Cpd.	Substituent R ¹	Substituent R ²	FLT3 ^(a) IC ₅₀ (μM)	PDGFR ^(b) IC ₅₀ (μM)
116 ^(d)	OCH ₃	H	> 30	> 30
117	OCH ₃	5'-F	> 30	> 30

Cpd.	FLT3 ^(a) IC ₅₀ (μM)	PDGFR ^(b) IC ₅₀ (μM)
1a	1.1	5.4

^a Assayed with endogenous FLT3 in EOL-1 cells. ^b Assayed with endogenous PDGFR in Swiss 3T3 fibroblasts. Consistent results were obtained for inhibition of FLT3 and PDGFR-β, overexpressed in HEK293 cells (not shown). ^c Previously published syntheses and results on PDGFR inhibition.¹² ^d Previously published synthesis.¹² [#] Selectivity significant with *p* < 0.05.

Scheme 2^a

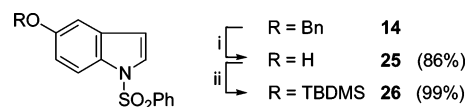
^a F: TBAF, THF, 60 °C or NaOH (10%), EtOH, 1:2, reflux. G: HCO₂NH₄, Pd/C, MeOH or THF/MeOH 1:1, 40–60 °C. H: NaH, DMF, 25 °C. I: NaOH, H₂O, 60 °C. J: KOH, (NH₂)₂, (CH₂OH)₂, microwave 200 W.

Scheme 3^a

^a i: DIBOC DMAP, MeCN. C: *t*-BuLi, THF, –78 °C. ii: (1) TBAF, THF, reflux; (2) TFA, DCM.

synthetic route shown in Scheme 1; protection of 7-ethyl-1*H*-indole was performed by the *tert*-butoxycarbonyl group¹⁵ instead of the phenylsulfonyl increment (Scheme 3). In case of $R^1 = \text{OBn}$ or $R^1 = R^2 = \text{OBn}$ hydrogenolytic cleavage of the benzyloxy group was then performed to obtain the phenolic compounds **98–109**.

After observation that Pd/C catalyzed benzyloxy deprotection of chloro-substituted bisindolylmethanones also leads to replace-

Scheme 4^a

^a i: Procedure G. ii: (1) NaH, THF; (2) TBDMSCl, 40 °C.

ment of halogen by hydrogen, we modified the synthetic route shown in Scheme 1 by use of the 2-lithiated species of the 5-(*tert*-butyldimethylsilyloxy)-1-phenylsulfonyl-1*H*-indole **26** for coupling with the 4-halo-1-phenylsulfonyl-1*H*-indole-2-carboxylic acid chlorides **39** and **41**. This leads to the *N*-phenylsulfonylated silyl ethers **69** and **70**, allowing access to compounds **110** and **111** by one-step alkaline complete deprotection (Scheme 2).

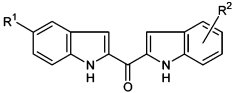
The ethers **112–115** bearing a polar alkoxy chain were synthesized from the corresponding 5-hydroxy derivatives **98**, **104**, and **107** by alkylation with *N,N*-dimethyl-2-chloroethylamine or 1-(2-chloroethyl)-piperidine.

The bisindolylmethanes **116**¹² and **117** were obtained by reduction of the carbonyl bridge of the corresponding bisindolylmethanones **4b**¹² and **78** using the Huang–Minlon modification¹⁶ of the Wolff–Kishner reaction.

Results and Discussion

The structures of the bisindolylmethanones and their IC₅₀ values for inhibition of FLT3 and PDGFR are shown in Table 1. The most potent FLT3 inhibitors **98** and **102** show a FLT3 IC₅₀ value of 0.06 and 0.04 μM, respectively. They are approximately 2 orders of magnitude more potent than the quinoxaline **1a**,^{17,18} which was tested as a reference compound. Interestingly, their inhibitory potency for PDGFR is about 1 order of magnitude lower (IC₅₀ = 0.96 and 0.30 μM, respectively). Another group of compounds is characterized by moderate but selective inhibition of PDGFR, notably compound **82**. Similar potency and selectivity data as in the cellular assays were obtained for the selected compounds **82**, **98**, **102**, and **113** when tested with recombinant kinases and an exogenous peptide substrate in cell-free assays. Also, the rank order of potency for the individual kinases could be reproduced in the *in vitro* assays. The data establish that differences in the cellular uptake and metabolism were not important for the observed selectivities of these compounds (Table 2).

A more detailed discussion of the SAR must be based on the probable binding mode and on the symmetry of the bis(1*H*-indol-2-yl)methanone scaffold. As suggested from a homology model of the PDGFR and from SAR of the previous, mainly monosubstituted bis(1*H*-indol-2-yl)methanone series,¹² the compounds may bind to the ATP site in a mode resembling the interaction of **118** (PD173074, 1-*tert*-butyl-3-[2-(4-diethylaminobutylamino)-6-(3,5-dimethoxyphenyl)-pyrido[2,3-*d*]pyrimidin-7-yl]-urea) in a crystallized complex with the FGFR-1.¹⁹ This mode is generally confirmed by the recent crystal structure (PDB 1rjb) of FLT3.¹⁴ The key interactions (see Figure 2) are two hydrogen bonds of an indole NH and the methanone oxygen with the CO and the NH moiety, respectively, of the backbone of FLT3 Cys-694 (PDGFR Cys-684). In contrast to the bisindolylmethanones **4b** and **78**, the bisindolylmethane homologues **116** and **117**, respectively, are inactive. Their methylene bridge between the indole moieties is incompatible with the putative binding mode. The bidentate hydrogen bond donor–acceptor system lets one indole ring point inward and the other outward and enables, by this, the definition of an inner and an outer binding pocket (see Figure 2B). The outer indole is open for substitution in positions 5 and 6 even with larger polar, e.g., piperidinoethoxy or quinolylcarboxy groups.¹² Whereas ether

Table 2. Inhibition of FLT3 and PDGFR Tyrosine Kinases by Selected Bis(1*H*-indol-2-yl)methanones in Cell-Free Assays^a


Cpd.	R ¹	R ²	hFLT3 IC ₅₀ ± SEM (μM)	hPDGFR-β IC ₅₀ ± SEM (μM)	Sig.
82	OCH ₃	6'-Cl	23.93 ± 6.08	0.055 ± 0.016	0.001
98	OH	4'-CH ₃	0.070 ± 0.024	0.458 ± 0.129	0.008
102	OH	5'-OH	0.033 ± 0.004	0.171 ± 0.043	0.005
113	2-piperidin-1-ylethoxy	4'-CH ₃	0.22 ± 0.019	1.20 ± 0.25	0.002

^a Assayed *in vitro* with recombinant kinase domains expressed as GST-fusion proteins in Sf9 cells, [³²Pγ]ATP, and an exogenous peptide substrate. The results are mean values ± standard error of the mean (SEM) of four independent titration experiments. Sig.: probability of error from two-tail Student's *t*-test of the pIC₅₀ difference between hFLT3 and hPDGFR-β.

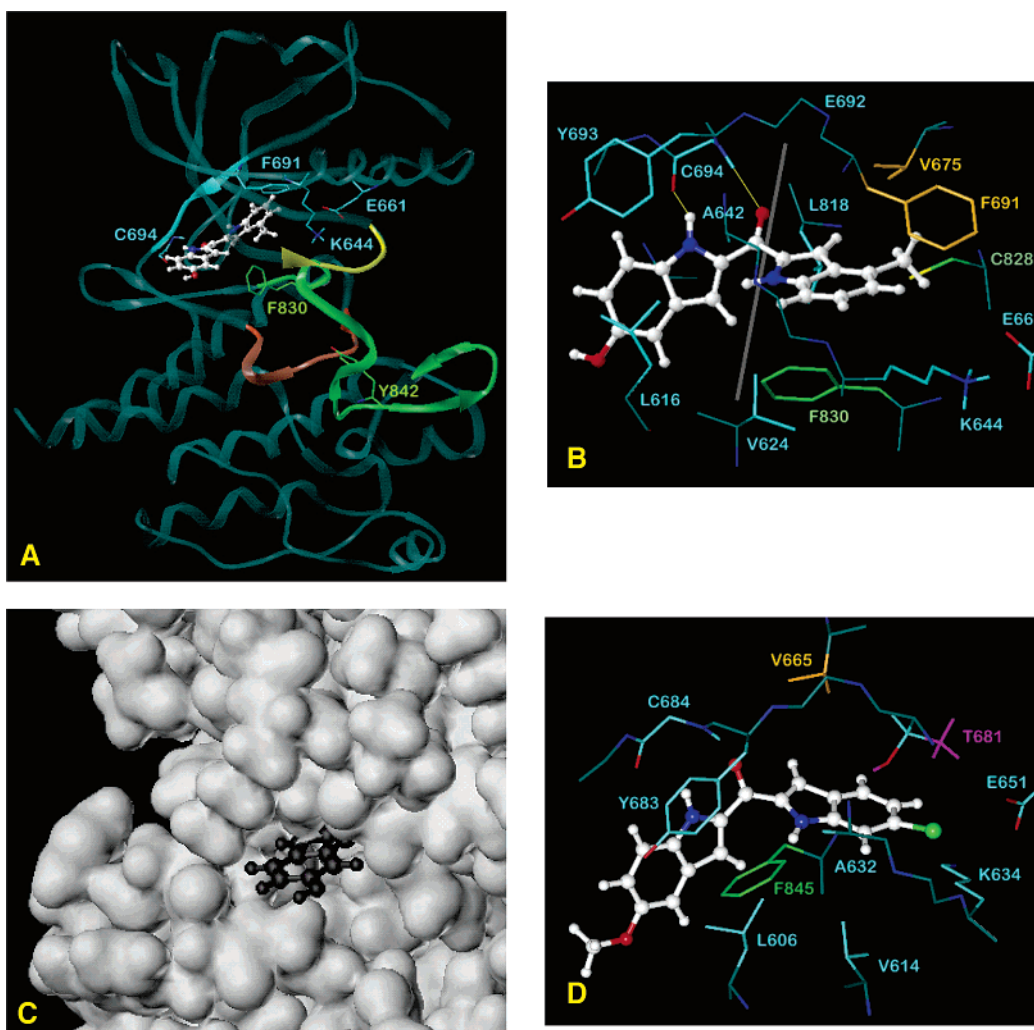


Figure 2. Suggested binding mode of **98** at FLT3 and **82** at PDGFR, demonstrated by minimized complexes with the FLT3 crystal structure 1rjb.¹⁴ (A) Overview of the model with **98** and with representation of some important amino acids. Specific regions are highlighted on the ribbon/tube backbone: light cyan, inhibitor binding site consisting of parts of β5 and the hinge region; yellow, nucleotide binding loop; red orange, catalytic loop; green, activation loop. (B) Detailed view of the binding site of **98** with all amino acids lying within a sphere of 3 Å around the ligand. Backbone atoms are dark, side chains light. C atoms orange, hydrophobic pocket (Phe-691, Val-675); C atoms green, activation loop residues. Yellow lines, hydrogen bonds of Cys-694 with the ligand. The gray line separates the inner (right) from the outer (left) binding pocket. (C) MOLCAD van der Waals surface of FLT3 with **98** in ball-and-stick representation. (D) Putative PDGFR binding site of **82** with all amino acids lying within a sphere of 3 Å around the ligand. The model was derived from the FLT3 crystal structure by mutation of the only different binding site residue, Phe-691, into PDGFR Thr-681 (side chain conformation like Thr-315 in the Abl kinase crystal structure 1iep²¹). Numbers of amino acids corresponding to hPDGFR-β. The side chain C and H atoms of Thr-681 are magenta, coloring of all other atoms such as in panel B.

substituents were not superior to 5-OH, PDGFR inhibition could be increased by ester moieties. The 5-substituents are surrounded by short chains of the β1 strand and of the hinge region and protrude into the solvent.

These general considerations will help to understand most of the SAR of the derivatives in Table 1 by suggesting which substituents probably belong to the inner and outer indole, respectively. Substituents in 4'-position should be inside the

pocket because of probable steric hindrance when present at the outer ring (see Figure 2). The FLT3 kinase seems to provide a specific interaction site especially for methyl in 4'-position. Compound **98** is significantly FLT3 selective in both cellular ($IC_{50} = 0.06 \mu\text{M}$ compared to $0.96 \mu\text{M}$ at PDGFR) and in vitro assays ($IC_{50} = 0.07 \mu\text{M}$ vs. $0.46 \mu\text{M}$, see Table 2). The 5-piperidinoethoxy-4'-methyl derivative **113**, FLT3 selective in both assays, too, confirms the inner position of the methyl since the large polar group must point outward. The 4'-halogen-substituted compounds **106**, **110**, and **111** are at least 10-fold less active at FLT3 than the methyl derivative **98** and unselective. The order of activity of the 4'-halogen groups is $F > Cl > Br$ (FLT3) and $Cl \geq F > Br$ (PDGFR), respectively. A 4'-methoxy group on its own has no effect on activity and selectivity (compare **3** and **72**). The hydroxy group in the 5-OH-4'-OMe derivative **103** increases inhibition of both kinases.

An important new insight is that a 5-OH group at the inner ring is favorable and may lead to FLT3 selectivity. The 5,5'-dihydroxy derivative **102** is the most active FLT3 inhibitor within the series (cellular $IC_{50} = 0.04 \mu\text{M}$, in vitro $IC_{50} = 0.033 \mu\text{M}$). The contributions of the hydroxy groups to FLT3 inhibition are similar and additive (ca. 1 order of magnitude, compare **3**, **4a**, and **102**). The data of the lead **3** indicate that the PDGFR incorporates an unsubstituted indole moiety into the inner pocket somewhat better than FLT3. Introduction of one 5-OH substituent (**4a**) increases PDGFR as well as FLT3 inhibition (5- and 8-fold, respectively). An additional hydroxy group in 5'-position does not further improve PDGFR activity (**102**). In conclusion, this different behavior of both kinases might be due to a favorable effect of a polar 5-substituent at the outer ring and to a specific FLT3 binding site for an inner 5'-hydroxy group.

Single 5-F substitution (**73**) reduces activity at both kinases by a factor of ca. 4 compared to 5-OH (**4a**). Fluorine may interact with the inner pocket as indicated by the data of the 5-methoxy, 5-benzyloxy, and 5-piperidinoethoxy derivatives **78**, **94**, and **115**, respectively. It should be noted that an about 10-fold reduction of PDGFR inhibition from 5-piperidinoethoxy to 5-benzyloxy compounds corresponds to the trend observed in similar monosubstituted analogues,¹⁴ i.e., larger substituents with polar termini are always superior to more hydrophobic groups. Taken together, the data of the compounds with small substituents such as F, OH, and Me in 5-position raise the question whether in some cases the measured IC_{50} values are based on a mixture of both binding orientations and/or even different modes at both kinases. For example, 5'-Me and 5'-F in the 5-OH compounds **99** and **107**, respectively, are generally able to fit in the inner and the outer pocket. It may be suggested that the more lipophilic moiety is preferentially transferred into the interior via hydrophobic patches.

A single 5-OMe group reduces FLT3 activity compared to 5-OH and leads to significant PDGFR selectivity (cf. **4a** and **4b**). An inner methoxy substituent in 5-position is unfavorable, since the 5,5'-di-OMe derivative has an IC_{50} of only about 10–30 μM at PDGFR.¹² All 5-OMe compounds with R^2 substituents at the other moiety are either unselective or PDGFR selective. In the 5'-halogen series, activity at both kinases decreases in the order of $F > Cl \geq Br$.

The 6-OMe derivative **5** is by a factor 3 to 5 more active than the unsubstituted lead **3**. The introduction of an additional 5-OH group at the other moiety does not significantly change activities (**104**). The 6'-substituted 5-OH derivatives **100**, **104**, and **108** are unselective and do not significantly differ in potency. Compounds **112** and **114** with large polar 5-substituents

indicate that a 6'-methoxy group may interact with the inner pocket without marked loss of potency. Interestingly, the 6'-substituted 5-OMe compounds are all significantly PDGFR selective. In the case of hydrophobic 6'-substituents such as methyl and chloro (**76** and **82**), the selectivity is even 20- to 40-fold because of the surprisingly high PDGFR and very weak FLT3 inhibition. For **82**, PDGFR selectivity was confirmed in vitro (see Table 2).

Together with a 5-OH group at the other ring, the 7'-substituted compounds **101**, **105**, and **109** are generally weakly active. Compound **83** (5-OMe-7'-Cl) is inactive at both kinases.

Modeling of the Putative Binding Mode. The PDB crystal structure 1rjb of FLT3¹⁴ offers the possibility to suggest interactions of bisindolylmethanones by docking into the ATP binding site. Figure 2 represents the final model with the highly active 5-OH-4'-Me derivative **98** as ligand. An overview of the binding site location is shown in panel A. The ligand fits to a bank of four residues, Phe-691 to Cys-694, belonging to $\beta 5$ and the hinge region. Within 3 Å around compound **98**, Phe-691 is the only mutated amino acid compared to the PDGFR (Thr-681) and, therefore, the primary candidate for explaining selectivity. Lys-644 ($\beta 3$) and Glu-661 (αC), forming a salt bridge as in other tyrosine kinases, are close to the 5-position of the inner indole ring. From the C-terminal domain, parts of $\beta 7$, $\beta 8$, and the DFG motif with Phe-830 make the bottom of the binding site. The course of the activation loop allows the fit of much larger ligands such as **2** (see Figure 1) which inhibits a FLT3 Phe-691-Thr mutant ($IC_{50} = 0.1\text{--}0.3 \mu\text{M}$ ²⁰). With respect to the whole Imatinib binding site, a FLT3 model mainly based on homology with the Abl kinase²⁰ was closely similar to the FLT3 crystal structure (rms distance of C α atoms 0.85 Å). Prerequisite of Imatinib activity is the inactive conformation of the activation loop, characterized by an autoinhibitory position of the unphosphorylated Tyr-842. The bis(1*H*-indol-2-yl)-methanones are not assumed to extend into the binding pocket like **2** because of the interaction with the backbone of Cys-694, which in the case of **2** forms a hydrogen bond with the terminal pyridine nitrogen. In the docking mode of **98**, neither the nucleotide binding nor the catalytic loop participate in binding.

The detailed interactions of compound **98** are shown in Figure 2B. In contrast to previous suggestions,¹² the conformation of the outer indole is synperiplanar (sp, cis) and of the inner indole antiperiplanar (ap, trans) based on the respective NC–CO torsion angle. Provided that the bidentate hydrogen bond exists, the FLT3 crystal structure has no specific counterpart for the inner indole NH function in both possible energy minima, sp/ap and sp/sp, but the 3-position is in hydrophobic contact with Val-675 in the sp/ap minimum conformation (see Figure 2). An additional H bond of the inner indole NH with the backbone oxygen of Glu-692 as suggested for PDGFR binding in sp/sp orientation¹² is impossible since then the 4'- and 7'-positions bump into the side chains of Phe-830 and Phe-691, respectively. AMPAC 6.55 calculations of **98** with the COSMO water solvation model result in the lowest energy for a sp/sp propeller-like conformation with NC–CO torsion angles of about 30/30 or –30/–30 degrees. However, the sp/ap minimum is only about 0.6 kcal/mol higher in energy, and the polar surface accessible to water is slightly larger. A reaction coordinate calculation of the rotation of the inner indole results in a barrier of only 2.2 kcal/mol. Therefore, each conformation is energetically possible in the bound state. However, a hydrophobic patch mainly consisting of Val-675, Phe-691, and Leu-818 appears to fit the

lipophilic edge of the inner indole (3- and 4-positions) and, therefore, to prefer the *sp/ap* conformation of the compounds.

The docking mode in Figure 2B explains the FLT3 selectivity of 4'-Me substituted derivatives by an about 3 Å distance of the methyl group to the phenyl plane of Phe-691, and also the hydrophobic interaction with Val-675 is optimal in case of 4'-Me. The lower FLT3 inhibition of the 4'-halogen substituted compounds **77**, **80**, **106**, **110** and **111** may be due to electrostatic repulsion with the π system of Phe-691. The 5'-position is directed toward the phenyl plane, too. In compound **102**, the 5'-OH group is 2.9 Å distant from the Phe-691 phenyl center, indicating that electrostatic interaction of the positively charged hydrogen with the π system contributes to the high FLT3 activity and selectivity. Generally, the 5'-OH substituent may also directly or via water interact with Lys-644 and Glu-661 ($\text{NH}_3^+ \dots \text{O}$ and $\text{CO}_2^- \dots \text{H}$ distances of ca. 4 Å). A 5'-Me substituent fits well to Phe-691, but not to Val-675. Insofar, the reduced activity of compound **99** corresponds to the given docking mode.

A polar group in 6-position may generally point into the solvent like a 5-substituent (see Figure 2A and C). Three of the compounds with a probable inner location of the 6'-substituent (**76**, **79** and **82**) are PDGFR selective. Comparing the data of the 5-OMe derivatives for both kinases, the 5'- and 6'-positions of all substituents except F seem to be nearly equivalent with respect to FLT3 activity, whereas the PDGFR prefers hydrophobic 6'-substituents such as methyl and chloro. The simplest hypothetic explanation for this rather unexpected finding may be given if the *sp/ap* binding mode is suggested for the PDGFR, too. Replacing FLT3 Phe-691 into the corresponding PDGFR Thr-681 with a conformation of the side chain like Thr-315 in the Abl kinase crystal structure *1iep*²¹ indicates interaction of the 6'-substituents with the methyl branch of Thr-681 (distance ca. 2.9 Å), whereas the OH hydrogen points to the indole ring (see Figure 2D). Contrariwise, larger groups in 5'-position like in compounds **75** and **84** clash with the threonine side chain.

Also the 7'-substituents rather belong to the inner indole ring. The FLT3 model indicates that bulky groups in this position should be sterically hindered especially by Val-624 and Ala-642. Compared to FLT3, the higher PDGFR activity of compounds **101**, **105**, and **109** cannot be explained without a more precise PDGFR model.

The binding site of the inner indole ring is completed by the side chains of Ala-642 (β 3) from the top and of Val-624 (β 2), Leu-818 (β 7), Cys-828 (β 8, also in contact with the 4'-Me group), and Phe-830 (DFG-motif) from the bottom. Additionally to the hydrogen bond with the Cys-694 backbone, the outer indole interacts with the N-terminal domain residues Leu-616 (β 1) and Tyr-693 (hinge) as well as with Phe-830. Figure 2C shows a volume representation of the binding site region, indicating how the outer indole moiety protrudes into the solvent. Obviously, the 5- and 6-positions are free and remain solvated in the bound state, whereas substituents in 4- and 7-positions should be sterically hindered. With this model, it becomes plausible that generally increased polarity (water solubility) and lower hydrophobicity of 5- and 6-substituents lead to higher activity at both kinases (compare 5-hydroxy with 5-methoxy, 5-benzyloxy with 5-piperidinoethoxy). Corresponding to previous results on PDGFR,¹² ether moieties in 5-position do not improve inhibition as compared to 5-hydroxy, and groups with polar termini like in compounds **112**–**115** are superior to derivatives with nonpolar ones.

In conclusion, the model in Figure 2 reasonably explains a lot of the structure–activity and structure–selectivity relation-

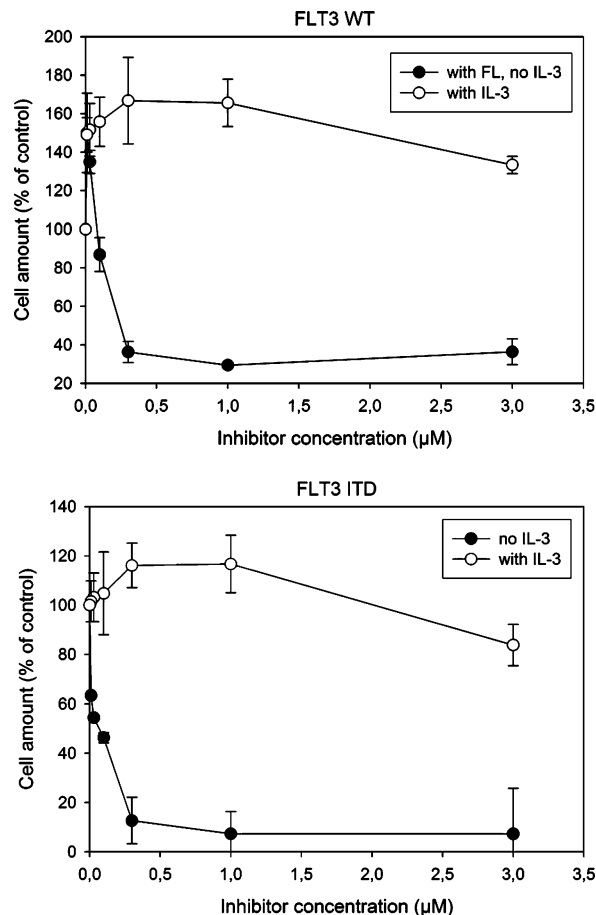


Figure 3. Inhibition of FLT3-dependent cell proliferation by the bis-(1*H*-indol-2-yl)methanone **102**. 32Dcl3 cells expressing wildtype FLT3 or FLT3-ITD (as indicated) were grown with different concentrations of the inhibitor in the absence or presence of FL or IL-3, as indicated, for 2 days. Cell amounts were subsequently determined with the MTT assay. Values are means \pm SD ($n = 6$). Note that very low concentrations of inhibitor sometimes led to stimulation of proliferation under these conditions.

ships of the bis(1*H*-indol-2-yl)methanone derivatives on a qualitative level, ascribing activity differences between FLT3 and PDGFR mainly to the Phe-Thr exchange. The symmetry of the scaffold and the similar energy of the minimum conformations actually suggest different binding orientations and conformations and even multiple modes of individual compounds and/or different modes at both kinases. It is, therefore, somewhat surprising that much of the data fit to a unique model. However, the lacking equivalence of the “inner” indole positions (4 and 7, 5 and 6), corresponds to a single binding mode.

Further Biological Tests. The most potent compound **102** was further explored for inhibition of FLT3-ITD in a cellular model of FLT3-driven proliferation. As depicted in Figure 3, proliferation of 32D cells in dependence on wild-type FLT3 or FLT3-ITD was inhibited with an activity (IC_{50} approximately 0.1 μM) close to that for FLT3 kinase inhibition in EOL-1 cells. IL-3 fully abolished inhibition, indicating that **102** is selective as it is not affecting kinases in the IL-3 signaling cascade. Equally potent inhibition of wild-type FLT3 and FLT3-ITD distinguishes compound **102** from other FLT3 inhibitors such as the indolocarbazole **1e**, which preferentially inhibit FLT3-ITD.²² Furthermore, compounds **98** and **102** potently induced apoptosis in primary blast cells obtained from AML patients (Figure 4, upper panels). All tested patient blasts contained wild-type FLT3 (data not shown), consistent with the capacity of **102** to block this version of FLT3. Thus, **102** and related bis-

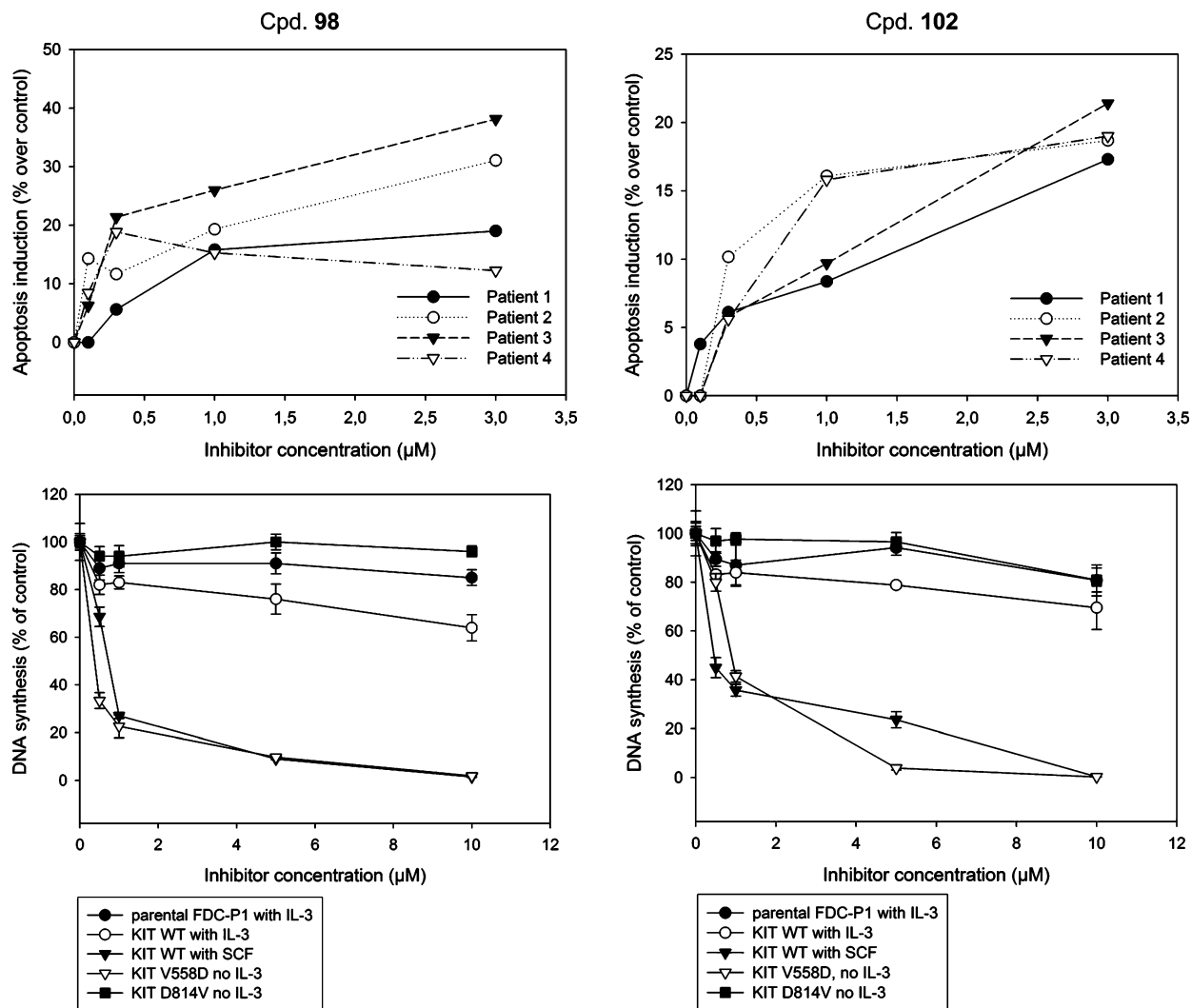


Figure 4. Activity of bisindolylmethanones in other biological assays. Apoptosis induction in primary human AML blasts by treatment with the bis(*1H*-indol-2-yl)methanones **98** (upper left panel) or **102** (upper right panel) for 72 h. The fraction of apoptotic cells was measured as Sub-G1 population by FACS analysis. Inhibition of c-Kit-dependent DNA synthesis in a FDC-P1 background by compound **98** (lower left panel) or **102** (lower right panel). Parental FDC-P1 cells or cell lines expressing different variants of KIT were treated for 42 h with the compounds in absence or presence of IL-3 or stem cell factor (SCF) as indicated. Subsequently, incorporation of [^3H]thymidine was determined.

(*1H*-indol-2-yl)methanones deserve further exploration as antitumor agents in AML.

Activating mutations in the KIT/stem cell factor (SCF) receptor have also been found in AML blasts,²³ and the KIT kinase domain is homologous to that of FLT3 and PDGFR. Therefore, the inhibition of KIT signaling activity by the most potent compounds **98** and **102** was tested, employing the IL-3-dependent FDC-P1 cells expressing either KIT wildtype or activated KIT mutants. As shown in Figure 4 (lower panels), KIT was generally less susceptible to inhibition than FLT3, with IC_{50} values ranging from approximately 0.5 μM with the KIT V558D mutant to 0.5–2 μM for wildtype KIT. The KIT D814V mutant was completely resistant to both compounds. A lower susceptibility of KIT for other members of this compound family has been observed by us earlier.¹³

Prompted by the high structural similarity of the ATP binding sites of FLT3 and the Abl-kinase, we also explored the inhibitory potency of selected bisindolylmethanones toward Abl. Potency for Abl inhibition of the bis(*1H*-indol-2-yl)methanones was, however, generally lower than for FLT3, exemplified by an IC_{50} for compound **102** of 1.3 μM for inhibition of recombinant Abl in vitro and 4.2 μM for inhibition of oncogenic Bcr-Abl kinase in K562 cells. Thus, Abl was 30- to 100-fold less sensitive to

inhibition by compound **102** than FLT3. Comparison of Abl crystal structures²¹ in complex with **2** and **119** (PD173955, 6-(2,6-dichlorophenyl)-8-methyl-2-(3-methylsulfanylphenylamino)-8*H*-pyrido[2,3-*d*]pyrimidin-7-one),²⁴ respectively, with FLT3 indicates that the conformations of the nucleotide binding loops are very different. In Abl, this loop is inwardly folded, approaching Tyr-253 (corresponding to FLT3 Phe-621) to the putative bisindolylmethanone binding site and constricting the available "inner" pocket. Thus, the Abl binding mode of the compounds may differ from that at FLT3. Anyway, the weaker activity at the Abl kinase is not uniquely due to the FLT3 Phe-691 Abl Thr-315 exchange, since also the PDGFR with the corresponding Thr-681 is more strongly inhibited than Abl by all tested derivatives (Table 1 and data not shown).

Conclusions

Bis(*1H*-indol-2-yl)methanones are a new family of potent FLT3 and PDGFR inhibitors. Despite the relatively small and simple scaffold, some compounds clearly exhibit selectivity among both kinases, depending on the substitution pattern. The most potent FLT3 inhibitors, compounds **98** and **102**, result in IC_{50} values of ca. 0.05 μM . Their potency for PDGFR is about 1 order of magnitude lower. In the case of 5-OMe and

hydrophobic 6'-substituents as in compounds **76** and **82**, 20- to 40-fold PDGFR selectivity is obtained. The putative binding mode at both kinases is based on a bidentate hydrogen bond of the outer indole NH and the methanone oxygen with the backbone of a cysteine residue in the hinge region. FLT3 activity and selectivity seem to depend on interactions of the inner indole moiety with a hydrophobic pocket including Val-675 and Phe-691, the only amino acid of the binding site which is different in the PDGFR kinase (Thr-681). Compound **102** potently inhibited wild-type FLT3 as well as FLT3-ITD-dependent proliferation of cells. Further structural optimization and further biological tests will help to investigate the role of bis(1*H*-indol-2-yl)methanones as potential drugs against tumors associated with constitutive FLT3 or PDGFR activation.

Experimental Section

Chemical Procedures. General. NMR spectra were recorded with a Bruker Avance 300 MHz spectrometer at 300 K, using TMS as an internal standard. IR spectra (KBr or pure solid) were measured with a Bruker Tensor 27 spectrometer. Melting points were determined with a Büchi B-545. MS spectra were measured with a Finnigan MAT 95 (EI, 70 eV). All reactions were carried out under nitrogen atmosphere. Elemental analyses were performed by the Analytical Lab. of the University of Regensburg.

Synthesis of 1-Phenylsulfonyl-1*H*-indoles. During 20 min, 60% NaH in paraffin (1.29 g, 43.0 mmol) was added to a stirred solution of the respective indole (42.0 mmol) in 60 mL of anhydrous THF at 0 °C. After stirring at room temperature for 1 h, benzenesulfonyl chloride (4.9 mL, 43.0 mmol) was added slowly. The reaction mixture was stirred for an additional 1 h and then poured into 500 mL of 5% aq. NaHCO₃ and extracted with ether (3 × 250 mL). The combined organic layers were dried (Na₂SO₄), and the solvent was removed under reduced pressure to give a beige solid. Recrystallization from ethanol afforded the title compound as colorless crystals.

1-Phenylsulfonyl-1*H*-indole²⁵ (6). Preparation from 1*H*-indole (Merck) as described above, Yield: 8.20 g (76%).

4-Methyl-1-phenylsulfonyl-1*H*-indole²⁶ (7). Preparation from 4-methyl-1*H*-indole (Acros) as described above, Yield: 51.44 g (89%).

5-Methyl-1-phenylsulfonyl-1*H*-indole²⁷ (8). Preparation from 5-methyl-1*H*-indole (Acros) as described above, Yield: 8.2 g (80%) colorless oil.

6-Methyl-1-phenylsulfonyl-1*H*-indole²⁸ (9). Preparation from 6-methyl-1*H*-indole (Acros) as described above, Yield: 6.9 g (71%).

4-Methoxy-1-phenylsulfonyl-1*H*-indole²⁹ (10). Preparation from 4-methoxy-1*H*-indole (Lancaster) as described above, Yield: 9.52 g (79%).

5-Methoxy-1-phenylsulfonyl-1*H*-indole³⁰ (11). Preparation from 5-methoxy-1*H*-indole (Acros) as described above, Yield: 7.12 g (89%).

6-Methoxy-1-phenylsulfonyl-1*H*-indole³⁰ (12). Preparation from 6-methoxy-1*H*-indole (Biosynth) as described above, Yield: 8.70 g (69%).

7-Methoxy-1-phenylsulfonyl-1*H*-indole³¹ (13). Preparation from 7-methoxy-1*H*-indole (Aldrich) as described above, Yield: 8.45 g (67%).

5-Benzyloxy-1-phenylsulfonyl-1*H*-indole¹² (14). Preparation from 5-benzyloxy-1*H*-indole (Lancaster) as described above, Yield: 19.72 g (87%).

4-Fluoro-1-phenylsulfonyl-1*H*-indole³² (15). Preparation from 4-fluoro-1*H*-indole (Aldrich) as described above, Yield: 7.74 g (67%).

5-Fluoro-1-phenylsulfonyl-1*H*-indole³³ (16). Preparation from 5-fluoro-1*H*-indole (Acros) as described above, Yield: 12.84 g (90%).

6-Fluoro-1-phenylsulfonyl-1*H*-indole (17). Preparation from 6-fluoro-1*H*-indole (Acros) as described above, Yield: 3.40 g (56%). Mp: 101.3–101.4 °C. Anal. (C₁₄H₁₀FNO₂S): C, H, N.

7-Fluoro-1-phenylsulfonyl-1*H*-indole (18). Preparation from 7-fluoro-1*H*-indole (Lancaster) as described above, Yield: 8.81 g (65%) beige crystals. Mp: 86–87 °C. Anal. (C₁₄H₁₀FNO₂S): C, H, N.

4-Chloro-1-phenylsulfonyl-1*H*-indole (19). Preparation from 4-chloro-1*H*-indole (Acros) as described above, Yield: 10.62 g (92%). Mp: 134–134.2 °C. Anal. (C₁₄H₁₀ClNO₂S): C, H, N.

5-Chloro-1-phenylsulfonyl-1*H*-indole³⁴ (20). Preparation from 5-chloro-1*H*-indole (Lancaster) as described above, Yield: 14.41 g (96%).

6-Chloro-1-phenylsulfonyl-1*H*-indole³⁵ (21). Preparation from 6-chloro-1*H*-indole (Lancaster) as described above, Yield: 7.1 g (70%).

7-Chloro-1-phenylsulfonyl-1*H*-indole (22). Preparation from 7-chloro-1*H*-indole (Lancaster) using DMF instead of THF as described above, Yield: 3.99 g (72%). Mp: 80–81 °C. Anal. (C₁₄H₁₀ClNO₂S): calcd. C 57.64, H 3.45, N 4.80; found C 58.31, H 3.86, N 4.81.

4-Bromo-1-phenylsulfonyl-1*H*-indole³² (23). Preparation from 4-bromo-1*H*-indole (Biosynth) as described above, Yield: 7.47 g (87%).

5-Bromo-1-phenylsulfonyl-1*H*-indole³⁶ (24). Preparation from 5-bromo-1*H*-indole (Lancaster) as described above, Yield: 12.29 g (87%).

Further N-Protected Indoles. 5-Hydroxy-1-phenylsulfonyl-1*H*-indole³¹ (25) was prepared from 5-benzyloxy-1-phenylsulfonyl-1*H*-indole **14** according to Procedure G (see below) in methanolic solution. Crystallization from dichloromethane/hexane yielded the product. Yield: 7.80 g (86%). Mp: 152.6–152.7 °C.

5-(*tert*-Butyldimethylsilyloxy)-1-phenylsulfonyl-1*H*-indole (26). During 20 min, 60% NaH in paraffin (2.20 g, 55.0 mmol) was added to a stirred solution of **25** (13.7 g, 50.0 mmol) in 750 mL of anhydrous THF at 25 °C. After stirring at room temperature for 1 h, *tert*-butyldimethylchlorosilane (8.29 g, 55.0 mmol) was added. The reaction mixture was stirred at 40 °C for an additional 1 h, the solvent removed in vacuo, the residue extracted with hot anhydrous hexane (2 × 100 mL), the hot suspension filtered over a pad of Na₂SO₄, and the product crystallized at –18 °C overnight. Yield: 19.18 g (99%). Mp: 77.8–78.8 °C. Anal. (C₂₀H₂₅NO₃-SSi): C, H, N.

7-Ethylindole-1-carboxylic Acid *tert*-Butyl Ester¹⁵ (27). Preparation from 7-ethyl-1*H*-indole (Acros) as follows: DMAP (0.52 g, 4.27 mmol) and di-*tert*-butyl dicarbonate (11.2 g, 51.24 mmol) were added to a 80 mL acetonitrile solution of the indole derivative (6.20 g, 42.7 mmol). The reaction mixture was then stirred till completion at room temperature (approximately 3 h, TLC control) before addition of 1.6 mL (15 mmol) of diethylamine. After 10 min of additional stirring, 80 mL of diethyl ether were poured into the mixture which was successively washed with a sat. potassium hydrogen sulfate aq. solution, water, and a sat. sodium hydrogen carbonate aq. solution. The organic phase was dried and evaporated. The crude product was subjected to column chromatography (SiO₂, petroleum ether/diethyl ether 3:1) to afford a light yellowish oil. Yield: 8.62 g (82%).

Procedure A: Preparation of (1-Phenylsulfonyl-1*H*-indol-2-yl)carbonic Acids. Metalation with *n*-Butyllithium. Method I: *n*-Butyllithium (1.6 M in hexane; 10.0 mL, 16.0 mmol) was added dropwise to a solution of the respective 1-phenylsulfonyl-1*H*-indole (15.0 mmol) in dry THF (50 mL) at –78 °C, to yield the respective (1*H*-indol-2-yl)lithium after stirring for 1 h. An excess of solid carbon dioxide was added, the mixture was warmed to room temperature, and the solvent was removed under reduced pressure. The white solid obtained was dissolved in water (100 mL) and the aqueous solution extracted with ethyl acetate (2 × 50 mL). The aqueous solution was separated, filtered, vigorously stirred, and acidified with concentrated HCl, yielding the respective carbonic acid. Crystallization from ethanol/water afforded an analytical pure sample. According to Method I the following carbonic acids were synthesized: 28–33.

Metalation with Lithiumdiisopropylamide (LDA). Method II: To a solution of the appropriate 1-phenylsulfonyl-1*H*-indole (15.0

mmol) in dry THF (100 mL) was added commercially available LDA (2 M solution in THF/*n*-heptane) at -78°C . After stirring for 1 h, an excess of solid carbon dioxide was added. The mixture was warmed to room temperature and the solvent removed under reduced pressure. To the white solid obtained, dichloromethane (about 3.0 mL per mmol) and hydrochloric acid (2 N, 1.0 mL/mmol) were added, and the mixture was refluxed for 1 h. The organic layer was washed with hydrochloric acid (2 N, 1.0 mL/mmol) and dried (Na_2SO_4). Removing the solvent under reduced pressure left an oily residue which was crystallized from diethyl ether. According to Method II the carboxylic acid **34** was synthesized.

1-Phenylsulfonyl-1H-indole-2-carboxylic Acid^{12,25} (**28**). Preparation according to Procedure A, Modification I. Yield: 7.3 g (79%) colorless crystals.

5-Methoxy-1-phenylsulfonyl-1H-indole-2-carboxylic Acid (**29**). Preparation according to Procedure A, Modification I. Yield: 32.5 g (91%) colorless crystals. Mp: 173.4–173.5 $^{\circ}\text{C}$. Anal. ($\text{C}_{16}\text{H}_{13}\text{NO}_5\text{S}$): calcd. C 58.00, H 3.95 N 4.23; found C 57.93, H 3.95, N 3.14.

5-Benzyloxy-1-phenylsulfonyl-1H-indole-2-carboxylic Acid¹² (**30**). Preparation according to Procedure A, Method I. Yield: 35.20 g (61%) colorless crystals.

5-Fluoro-1-phenylsulfonyl-1H-indole-2-carboxylic Acid (**31**). Preparation according to Procedure A, Modification I. Yield: 3.49 g (57%) colorless crystals. Mp: 190–192 $^{\circ}\text{C}$. Anal. ($\text{C}_{15}\text{H}_{10}\text{FNO}_4\text{S}$): C, H, N.

4-Chloro-1-phenylsulfonyl-1H-indole-2-carboxylic Acid (**32**). Preparation according to Procedure A, Modification I. Yield: 5.93 g (84%) colorless crystals. Mp: 164–164.2 $^{\circ}\text{C}$. Anal. ($\text{C}_{15}\text{H}_{10}\text{ClNO}_4\text{S}$): C, H, N.

6-Chloro-1-phenylsulfonyl-1H-indole-2-carboxylic Acid (**33**). Preparation according to Procedure A, Modification I. Yield: 5.03 g (63%) colorless crystals. Mp: 139–140 $^{\circ}\text{C}$. Anal. ($\text{C}_{15}\text{H}_{10}\text{ClNO}_4\text{S}$): C, H, N.

4-Bromo-1-phenylsulfonyl-1H-indole-2-carboxylic Acid (**34**). Preparation according to Procedure A, Modification II. Yield: 4.49 g (63%) colorless crystals. Mp: 173.5–174 $^{\circ}\text{C}$. Anal. ($\text{C}_{15}\text{H}_{10}\text{BrNO}_4\text{S}$): C, H, N.

Procedure B: Preparation of 1-Phenylsulfonyl-1H-indole-2-carbonyl Chlorides. The appropriate 1-phenylsulfonyl-1H-indole-2-carboxylic acid (5.0 mmol) was dissolved in thionyl chloride (10.0 mL) and refluxed for 1 h. Excess of thionyl chloride was removed under reduced pressure, and the acid chloride was dried in vacuo. **35–41** were used for further synthesis without purification. Analytical samples could be obtained by column chromatography (SiO_2 , DCM) and crystallization from DCM/hexane.

1-Phenylsulfonyl-1H-indole-2-carbonyl Chloride¹² (**35**). Yield: 3.24 g (99%) colorless crystals.

5-Methoxy-1-phenylsulfonyl-1H-indole-2-carbonyl Chloride (**36**). Yield: 14.82 g (99%). Mp: 146.3–146.4 $^{\circ}\text{C}$. Anal. ($\text{C}_{16}\text{H}_{12}\text{ClNO}_4\text{S}$): C, H, N.

5-Benzyloxy-1-phenylsulfonyl-1H-indole-2-carbonyl Chloride¹² (**37**). Yield: 7.83 g (99%) beige crystals.

5-Fluoro-1-phenylsulfonyl-1H-indole-2-carbonyl Chloride (**38**). Yield: 3.46 g (99%). Mp: 125–130 $^{\circ}\text{C}$. Anal. ($\text{C}_{15}\text{H}_9\text{ClFNO}_3\text{S}$): C, H, N.

4-Chloro-1-phenylsulfonyl-1H-indole-2-carbonyl Chloride (**39**). Yield: 3.31 g (99%). Mp: 151–156 $^{\circ}\text{C}$. Anal. ($\text{C}_{15}\text{H}_9\text{Cl}_2\text{NO}_3\text{S}$): C, H, N.

6-Chloro-1-phenylsulfonyl-1H-indole-2-carbonyl Chloride (**40**). Yield: 3.92 g (99%). Mp: 204.2–204.3 $^{\circ}\text{C}$. Anal. ($\text{C}_{15}\text{H}_9\text{Cl}_2\text{NO}_3\text{S}$): C, H, N.

4-Bromo-1-phenylsulfonyl-1H-indole-2-carbonyl Chloride (**41**). Yield: 3.87 g (99%). Mp: 161–162 $^{\circ}\text{C}$. Anal. ($\text{C}_{15}\text{H}_9\text{BrClNO}_3\text{S}$): C, H, N.

Procedure C: Preparation of N-protected Bis(1H-indol-2-yl)methanones (45–70) and -methanole (43). At -78°C to a solution of the appropriate N-protected (1H-indol-2-yl)lithium (5.0 mmol) (cf. Procedure A) was added the respective (1-phenylsulfonyl-1H-indol-2-yl)carbonic acid chloride **35–41** (cf. Procedure B)

respective the aldehyde **42** (5.5 mmol) (cf. Procedure D) in THF. The mixture was allowed to warm to room-temperature overnight, hydrolyzed with 300 mL 2% aq. NaHCO_3 , and extracted with CH_2Cl_2 (3×50 mL), and the combined organic layers were dried (Na_2SO_4). Column chromatography (SiO_2 , CH_2Cl_2) and crystallization from diethyl ether/light petrol (4:1) afforded the product as colorless to faintly yellowish crystals.

(4-Methoxy-1-phenylsulfonyl-1H-indol-2-yl)-(1-phenylsulfonyl-1H-indol-2-yl)methanone (**43**). Metalation of **10** was performed according to procedure A, Method II. Yield: 5.83 g (73%). Mp: 86–89 $^{\circ}\text{C}$. Anal. ($\text{C}_{30}\text{H}_{24}\text{N}_2\text{O}_6\text{S}_2$): C, H, N.

(5-Fluoro-1-phenylsulfonyl-1H-indol-2-yl)-(1-phenylsulfonyl-1H-indol-2-yl)methanone (**45**). Metalation of **16** was performed according to Procedure A, Method II. Yield: 0.78 g (26%). Mp: 220.0–221.3 $^{\circ}\text{C}$. Anal. ($\text{C}_{29}\text{H}_{19}\text{FN}_2\text{O}_5\text{S}_2$): C, H, N.

(5-Methoxy-1-phenylsulfonyl-1H-indol-2-yl)-(4-methyl-1-phenylsulfonyl-1H-indol-2-yl)methanone (**46**). Metalation of **7** was performed according to Procedure A, Method II. Yield: 1.02 g (47%). Mp: 214.7–214.9 $^{\circ}\text{C}$. Anal. ($\text{C}_{31}\text{H}_{24}\text{N}_2\text{O}_6\text{S}_2$): C, H, N.

(5-Methoxy-1-phenylsulfonyl-1H-indol-2-yl)-(5-methyl-1-phenylsulfonyl-1H-indol-2-yl)methanone (**47**). Metalation of **8** was performed according to Procedure A, Method I. Yield: 1.30 g (38%). Mp: 208–209 $^{\circ}\text{C}$. Anal. ($\text{C}_{31}\text{H}_{24}\text{N}_2\text{O}_6\text{S}_2$): calcd. C 63.68, H 4.14, N 4.79; found C 63.11, H 4.22, N 4.85.

(5-Methoxy-1-phenylsulfonyl-1H-indol-2-yl)-(6-methyl-1-phenylsulfonyl-1H-indol-2-yl)methanone (**48**). Metalation of **12** was performed according to Procedure A, Method I. Yield: 0.89 g (29%). Mp: 194–195 $^{\circ}\text{C}$. Anal. ($\text{C}_{31}\text{H}_{24}\text{N}_2\text{O}_6\text{S}_2$): C, H, N.

(4-Fluoro-1-phenylsulfonyl-1H-indol-2-yl)-(5-methoxy-phenylsulfonyl-1H-indol-2-yl)methanone (**49**). Metalation of **15** was performed according to Procedure A, Method I. Yield: 1.52 g (36%). Mp: 223–224 $^{\circ}\text{C}$. Anal. ($\text{C}_{30}\text{H}_{21}\text{FN}_2\text{O}_6\text{S}_2$): C, H, N.

(5-Fluoro-1-phenylsulfonyl-1H-indol-2-yl)-(5-methoxy-1-phenylsulfonyl-1H-indol-2-yl)methanone (**50**). Metalation of **16** was performed according to Procedure A, Method II. Yield: 1.20 g (38%). Mp: 179.4–182.9 $^{\circ}\text{C}$. Anal. ($\text{C}_{30}\text{H}_{21}\text{FN}_2\text{O}_6\text{S}_2$): C, H, N.

(6-Fluoro-1-phenylsulfonyl-1H-indol-2-yl)-(5-methoxy-1-phenylsulfonyl-1H-indol-2-yl)methanone (**51**). Metalation of **17** was performed according to Procedure A, Method II. Yield: 0.85 g (40%). Mp: 224.3–226.5 $^{\circ}\text{C}$. Anal. ($\text{C}_{30}\text{H}_{21}\text{FN}_2\text{O}_6\text{S}_2$): C, H, N.

(4-Chloro-1-phenylsulfonyl-1H-indol-2-yl)-(5-methoxy-phenylsulfonyl-1H-indol-2-yl)methanone (**52**). Metalation of **19** was performed according to Procedure A, Method I. Yield: 2.59 g (63%). Mp: 239–240 $^{\circ}\text{C}$. Anal. ($\text{C}_{30}\text{H}_{21}\text{ClN}_2\text{O}_6\text{S}_2$): C, H, N.

(5-Chloro-1-phenylsulfonyl-1H-indol-2-yl)-(5-methoxy-1-phenylsulfonyl-1H-indol-2-yl)methanone (**53**). Metalation of **20** was performed according to Procedure A, Method II. Yield: 1.46 g (47%). Mp: 186.9–188.7 $^{\circ}\text{C}$. Anal. ($\text{C}_{30}\text{H}_{21}\text{ClN}_2\text{O}_6\text{S}_2$): C, H, N.

(6-Chloro-1-phenylsulfonyl-1H-indol-2-yl)-(5-methoxy-1-phenylsulfonyl-1H-indol-2-yl)methanone (**54**). Metalation of **11** was performed according to Procedure A, Method I. Yield: 1.44 g (40%). Mp: dec 186–187 $^{\circ}\text{C}$. Anal. ($\text{C}_{30}\text{H}_{21}\text{ClN}_2\text{O}_6\text{S}_2$): C, H, N.

(7-Chloro-1-phenylsulfonyl-1H-indol-2-yl)-(5-methoxy-1-phenylsulfonyl-1H-indol-2-yl)methanone (**55**). Metalation of **22** was performed according to Procedure A, Method I. Yield: 0.89 g (28%). Mp: 199.0–199.3 $^{\circ}\text{C}$. Anal. ($\text{C}_{30}\text{H}_{21}\text{ClN}_2\text{O}_6\text{S}_2$): C, H, N.

(5-Bromo-1-phenylsulfonyl-1H-indol-2-yl)-(5-methoxy-1-phenylsulfonyl-1H-indol-2-yl)methanone (**56**). Metalation of **24** was performed according to Procedure A, Method II. Yield: 0.64 g (80%). Mp: 259.9–251.0 $^{\circ}\text{C}$. Anal. ($\text{C}_{30}\text{H}_{12}\text{BrN}_2\text{O}_6\text{S}_2$): C, H, N.

(5-Fluoro-1-phenylsulfonyl-1H-indol-2-yl)-(4-methyl-1-phenylsulfonyl-1H-indol-2-yl)methanone (**57**). Metalation of **7** was performed according to Procedure A, Method II. Yield: 1.08 g (51%). Mp: 214.9–217.1 $^{\circ}\text{C}$. Anal. ($\text{C}_{30}\text{H}_{21}\text{FN}_2\text{O}_5\text{S}_2$): C, H, N.

(5-Benzyloxy-1-phenylsulfonyl-1H-indol-2-yl)-(4-methyl-1-phenylsulfonyl-1H-indol-2-yl)methanone (**58**). Metalation of **7** was performed according to Procedure A, Method II. Yield: 2.12 g (36%). Mp: 207–208 $^{\circ}\text{C}$. Anal. ($\text{C}_{37}\text{H}_{28}\text{N}_2\text{O}_6\text{S}_2$): C, H, N.

(5-Benzyloxy-1-phenylsulfonyl-1H-indol-2-yl)-(5-methyl-1-phenylsulfonyl-1H-indol-2-yl)methanone (**59**). Metalation of **8**

was performed according to Procedure A, Method I. Yield: 4.38 g (33%). Mp: 141–143 °C. Anal. (C₃₇H₂₈N₂O₆S₂): C, H, N.

(5-Benzoyloxy-1-phenylsulfonyl-1H-indol-2-yl)-(6-methyl-1-phenylsulfonyl-1H-indol-2-yl)methanone (60). Metalation of **9** was performed according to Procedure A, Method I. Yield: 8.34 g (75%). Mp: 203 °C. Anal. (C₃₇H₂₈N₂O₆S₂): C, H, N.

Bis-(5-benzoyloxy-1-phenylsulfonyl-1H-indol-2-yl)methanone (61). Metalation of **14** was performed according to Procedure A, Method I. Yield: 3.37 g (41%). Mp: 179.5–180 °C. Anal. (C₄₃H₃₂N₂O₇S₂): C, H, N.

(5-Benzoyloxy-1-phenylsulfonyl-1H-indol-2-yl)-(4-methoxy-1-phenylsulfonyl-1H-indol-2-yl)methanone (62). Metalation of **10** was performed according to Procedure A, Method I. Yield: 5.90 g (58%). Mp: 190–192 °C. Anal. (C₃₇H₂₈N₂O₇S₂): C, H, N.

(5-Benzoyloxy-1-phenylsulfonyl-1H-indol-2-yl)-(6-methoxy-1-phenylsulfonyl-1H-indol-2-yl)methanone (63). Metalation of **12** was performed according to Procedure A, Method II. Yield: 9.49 g (49%). Mp: 208.1–209.5 °C. Anal. (C₃₇H₂₈N₂O₇S₂): C, H, N.

(5-Benzoyloxy-1-phenylsulfonyl-1H-indol-2-yl)-(7-methoxy-1-phenylsulfonyl-1H-indol-2-yl)methanone (64). Metalation of **13** was performed according to Procedure A, Method I. Yield: 10.62 g (61%). Mp: 146.1–146.3 °C. Anal. (C₃₇H₂₈N₂O₇S₂): C, H, N.

(5-Benzoyloxy-1-phenylsulfonyl-1H-indol-2-yl)-(4-fluoro-1-phenylsulfonyl-1H-indol-2-yl)methanone (65). Metalation of **15** was performed according to Procedure A, Method II. Yield: 1.98 g (32%). Mp: dec 135 °C. Anal. (C₃₆H₂₅FN₂O₆S₂): C, H, N.

(5-Benzoyloxy-1-phenylsulfonyl-1H-indol-2-yl)-(5-fluoro-1-phenylsulfonyl-1H-indol-2-yl)methanone (66). Metalation of **16** was performed according to Procedure A, Method II. Yield: 7.01 g (55%). Mp: 237.1–237.6 °C. Anal. (C₃₆H₂₅FN₂O₆S₂): calcd. C 65.05, H 3.79, N 4.21; found C 64.42, H 4.20, N 3.80.

(5-Benzoyloxy-1-phenylsulfonyl-1H-indol-2-yl)-(6-fluoro-1-phenylsulfonyl-1H-indol-2-yl)methanone (67). Metalation of **17** was performed according to Procedure A, Method II. Yield: 1.48 g (25%). Mp: 196.2–196.7 °C. Anal. (C₃₆H₂₅FN₂O₆S₂): C, H, N.

(5-Benzoyloxy-1-phenylsulfonyl-1H-indol-2-yl)-(7-fluoro-1-phenylsulfonyl-1H-indol-2-yl)methanone (68). Metalation of **18** was performed according to Procedure A, Method I. Yield: 2.18 g (20%). Mp: 146.1–146.3 °C. Anal. (C₃₆H₂₅FN₂O₆S₂): C, H, N.

(5-(tert-Butyldimethylsilyloxy)-1-phenylsulfonyl-1H-indol-2-yl)-(4-chloro-1-phenylsulfonyl-1H-indol-2-yl)methanone (69). Metalation of **26** was performed according to Procedure A, Method I. Yield: 4.70 g (64%). Mp: 183–184 °C. Anal. (C₃₅H₃₃ClN₂O₆S₂-Si): C, H, N.

(4-Bromo-1-phenylsulfonyl-1H-indol-2-yl)-(5-(tert-butylidimethylsilyloxy)-1-phenylsulfonyl-1H-indol-2-yl)methanone (70). Metalation of **26** was performed according to Procedure A, Method I. Yield: 2.85 g (43%). Mp: 167.6–167.7 °C. Anal. (C₃₅H₃₃-BrN₂O₆S₂Si): C, H, N.

2-(1-Phenylsulfonyl-5-benzoyloxy-1H-indole-2-carbonyl)-7-ethylindole-1-carboxylic Acid tert-butyl ester (71). Metalation of **27** was performed with 1.02 eq of *tert*-Butyllithium (1.5 M in Pentane). Yield: 2.25 g (64%). Mp: 78–82 °C. Anal. (C₃₇H₃₄N₂O₆S): C, H, N.

Procedure D: Preparation of 2-formyl-1-phenylsulfonyl-1H-indoles. To a solution of the respective 1-phenylsulfonyl-1H-indole (15.0 mmol) in dry THF (100 mL) was added commercially available LDA (2M solution in THF/*n*-heptane) at –78 °C. After stirring for 1 h at room temperature, the solution was cooled again to –78 °C and DMF (30.0 mmol) added dropwise. Once more the solution was stirred at room temperature for 1 h and then poured on 40 mL of a saturated aqueous ammonium chloride solution. After extraction with ethyl acetate, the combined organic layers were dried over magnesium sulfate and evaporated under reduced pressure. The oily residue thus obtained was crystallized by addition of diethyl ether, removed by filtration, and washed with petroleum ether.

1-Phenylsulfonyl-1H-indol-2-yl carbaldehyde (42). Preparation from 1-phenylsulfonyl-1H-indole **6** as described above. Yield: 13 g (76%). Mp: 143.0–143.5 °C (lit.³⁷ Mp 111–111.5°C).

Procedure E: Preparation of Bis(1-phenylsulfonyl-1H-indolyl)methanones by Oxidation of Their Respective Carbinols.

PDC (pyridinium dichromate) (11.66 g, 31.0 mmol) and PTFA (pyridinium trifluoroacetate) (2.48 g, 155 mmol) were added to a solution of bis(1-phenylsulfonyl-1H-indol-2-yl)methanone (6.2 mmol) in 40 mL of dry CH₂Cl₂. When the oxidation was completed (2 to 12 h, TLC control), solid chromium waste was removed by filtration through SiO₂. Evaporation of the solvent left a foamy material which was purified by column chromatography on silica gel with DCM as eluent leading to light yellow crystals.

(1-Phenylsulfonyl-1H-indol-2-yl)-(4-methoxy-1-phenylsulfonyl-1H-indol-2-yl)methanone (44). Preparation from the N-phenylsulfonated methanone derivative **43** as described above. Yield: 2.05 g (58%). Mp: 176–177 °C. Anal. (C₃₀H₂₂N₂O₆S₂): C, H, N.

Procedure F: Removal of the Phenylsulfonyl Protection Group. Formation of Bis(1H-indol-2-yl)methanones. Cleavage with TBAF. Method I: A mixture of a N-protected methanone derivative (1.8 mmol) and TBAF (tetrabutylammonium fluoride trihydrate) (1.14 g, 3.6 mmol) in THF (30 mL) was gently refluxed. When TLC indicated that the reaction was completed (30 min to 12 h), the mixture was poured into water (250 mL) and extracted with ethyl acetate (3 × 50 mL), the organic layer dried (Na₂SO₄), and a part of the solvent removed to allow precipitation of the yellow product. According to this method compounds **73–96** were prepared.

Cleavage with NaOH Solution. Method II: The N-protected methanone derivative (1.8 mmol) was heated in ethanol (40 mL) and 10% aq. NaOH (20 mL) under reflux for 12 h. After cooling, the solution was poured into brine (100 mL) and extracted with ethyl acetate (3 × 50 mL). The combined organic layers were dried (Na₂SO₄) and evaporated under reduced pressure to leave the crude product, which was subjected to column chromatography (SiO₂, CH₂Cl₂). Method II was used for preparation of compound **72**.

(1H-Indol-2-yl)-(4-methoxy-1H-indol-2-yl)methanone (72). Yield: 0.30 g (85%). Mp: 200 °C. Anal. (C₁₈H₁₄N₂O₂): C, H, N.

(5-Fluoro-1H-indol-2-yl)-(1H-indol-2-yl)methanone (73). Yield: 0.32 g (55%). Mp: 252.8–253.3 °C. Anal. (C₁₇H₁₁FN₂O): C, H, N.

(5-Methoxy-1H-indol-2-yl)-(4-methyl-1H-indol-2-yl)methanone (74). Yield: 0.22 g (48%). Mp: 209.0–213.7 °C. Anal. (C₁₉H₁₆N₂O₂): C, H, N.

(5-Methoxy-1H-indol-2-yl)-(5-methyl-1H-indol-2-yl)methanone (75). Yield: 0.46 g (88%). Mp: 296 °C. Anal. (C₁₉H₁₆N₂O₂): C, H, N.

(5-Methoxy-1H-indol-2-yl)-(6-methyl-1H-indol-2-yl)methanone (76). Yield: 0.14 g (50%). Mp: 228.5–229 °C. Anal. (C₁₉H₁₆N₂O₂): C, H, N.

(4-Fluoro-1H-indol-2-yl)-(5-Methoxy-1H-indol-2-yl)methanone (77). Yield: 0.09 g (19%). Mp: 194–195 °C. Anal. (C₁₈H₁₃FN₂O₂): C, H, N.

(5-Fluoro-1H-indol-2-yl)-(5-methoxy-1H-indol-2-yl)methanone (78). Yield: 0.17 g (34%). Mp: 187.8–187.9 °C. Anal. (C₁₈H₁₃FN₂O₂): C, H, N.

(6-Fluoro-1H-indol-2-yl)-(5-methoxy-1H-indol-2-yl)methanone (79). Yield: 0.10 g (28%). Mp: 207.8–209.2 °C. Anal. (C₁₈H₁₃FN₂O₂·1/6 CH₂Cl₂): C, H, N.

(4-Chloro-1H-indol-2-yl)-(5-methoxy-1H-indol-2-yl)methanone (80). Yield: 0.7 g (39%). Mp: 236.5–237 °C. Anal. (C₁₈H₁₃ClN₂O₂): C, H, N.

(5-Chloro-1H-indol-2-yl)-(5-methoxy-1H-indol-2-yl)methanone (81). Yield: 0.15 g (48%). Mp: 221.8–221.9 °C. Anal. (C₁₈H₁₃ClN₂O₂): C, H, N.

(6-Chloro-1H-indol-2-yl)-(5-methoxy-1H-indol-2-yl)methanone (82). Yield: 0.25 g (42%). Mp: 228.5–229 °C. Anal. (C₁₈H₁₃ClN₂O₂): C, H, N.

(7-Chloro-1H-indol-2-yl)-(5-methoxy-1H-indol-2-yl)methanone (83). Yield: 0.16 g (47%). Mp: 228.6–229.2 °C. Anal. (C₁₈H₁₃ClN₂O₂): C, H, N.

(5-Bromo-1H-indol-2-yl)-(5-methoxy-1H-indol-2-yl)methanone (84). Yield: 0.16 g (70%). Mp: 227.9–228.3 °C. Anal. (C₁₈H₁₃BrN₂O₂): calcd. C, H, N.

(5-Fluoro-1*H*-indol-2-yl)-(4-methyl-1*H*-indol-2-yl)methanone (85). Yield: 0.18 g (45%). Mp: 240.9–241.4 °C. Anal. (C₁₈H₁₃FN₂O): C, H, N.

(5-Benzyloxy-1*H*-indol-2-yl)-(4-methyl-1*H*-indol-2-yl)methanone (86). Yield: 0.53 g (92%). Mp: 236–237 °C. Anal. (C₂₅H₂₀N₂O₂): calcd. C 78.93, H 5.30, N 7.36; found C 78.08, H 5.24, N 7.20.

(5-Benzyloxy-1*H*-indol-2-yl)-(5-methyl-1*H*-indol-2-yl)methanone (87). Yield: 1.5 g (74%). Mp: 196–197 °C. Anal. (C₂₅H₂₀N₂O₂): C, H, N.

(5-Benzyloxy-1*H*-indol-2-yl)-(6-methyl-1*H*-indol-2-yl)methanone (88). Yield: 0.60 g (84%). Mp: 94 °C. Anal. (C₂₅H₂₀N₂O₂): calcd. C 78.93, H 5.30, N 7.36; found C 78.42, H 5.36, N 7.22.

Bis-(5-benzyloxy-1*H*-indol-2-yl)methanone (89). Yield: 1.12 g (62%). Mp: 192.5–193 °C. Anal. (C₃₁H₂₄N₂O₃): C, H, N.

(5-Benzyloxy-1*H*-indol-2-yl)-(4-methoxy-1*H*-indol-2-yl)methanone (90). Yield: 2.16 g (81%). Mp: 239–240 °C. Anal. (C₂₅H₂₀N₂O₃): C, H, N.

(5-Benzyloxy-1*H*-indol-2-yl)-(6-methoxy-1*H*-indol-2-yl)methanone (91). Yield 3.25 g (63%). Mp: 198.9–199.0 °C. Anal. (C₂₅H₂₀N₂O₃): C, H, N.

(5-Benzyloxy-1*H*-indol-2-yl)-(7-methoxy-1*H*-indol-2-yl)methanone (92). Yield: 2.37 g (48%). Mp: 201.0–201.8 °C. Anal. (C₂₅H₂₀N₂O₃): C, H, N.

(5-Benzyloxy-1*H*-indol-2-yl)-(4-fluoro-1*H*-indol-2-yl)methanone (93). Yield: 0.24 g (67%). Mp: 224 °C. Anal. (C₂₄H₁₇FN₂O₂): C, H, N.

(5-Benzyloxy-1*H*-indol-2-yl)-(5-fluoro-1*H*-indol-2-yl)methanone (94). Yield: 2.63 g (69%). Mp: 245.3–246.3 °C. Anal. (C₂₄H₁₇FN₂O₂): C, H, N.

(5-Benzyloxy-1*H*-indol-2-yl)-(6-fluoro-1*H*-indol-2-yl)methanone (95). Yield: 0.62 g (57%). Mp: 216.5–216.6 °C. Anal. (C₂₄H₁₇FN₂O₂): C, H, N.

(5-Benzyloxy-1*H*-indol-2-yl)-(7-fluoro-1*H*-indol-2-yl)methanone (96). Yield: 0.20 g (22%). Mp: dec 249 °C. Anal. (C₂₄H₁₇FN₂O₂): calcd. C 74.99, H 4.46, N 7.29; found C 74.22, H 4.48, N 7.08.

Consecutive Phenylsulfonyl and tert-Butoxycarbonyl Protection Groups Cleavage Leading to the Bisindolylmethanone Derivative (97). A THF solution (50 mL) of **71** (2.0 g, 3.15 mmol) and TBAF (4 g) was heated to reflux for 3 h. The solution was then poured into 500 mL of water, followed by extraction with dichloromethane. The combined organic layers were dried over sodium sulfate and filtered before addition of trifluoroacetic acid (20 mL). Additional stirring for 18 h of the reaction mixture was followed by hydrolysis with a saturated sodium hydrogen carbonate solution. Separation of the organic layer and evaporation of the solvent led to the crude product which was purified by column chromatography (SiO₂, dichloromethane/ethyl acetate 10:1).

(5-Benzyloxy-1*H*-indol-2-yl)-(7-ethyl-1*H*-indol-2-yl)methanone (97). Yield: 0.72 g of a foam (58%). Mp: 162–165 °C. Anal. (C₂₆H₂₂N₂O₂): calcd. C 79.16, H 5.62, N 7.10; found C 78.88, H 6.06, N 6.71.

Procedure G: Hydrogenolytic Preparation of Hydroxymethanones. A mixture of the respective benzyloxy compound **86–97** (10.92 mmol), ammonium formate (12.00 g, 188.80 mmol), and 5–10% Pd/C (2.0 g) in 1:1 (v/v) methanol/THF (200 mL) was stirred at 40 to 60 °C for 4 h. After removing the catalyst, the solvent was evaporated to leave an oily material. Ethyl acetate (200 mL) and water (100 mL) were added. The organic layer was washed with water and dried (Na₂SO₄), and the solvent was evaporated. Treatment of the residue with a little diethyl ether results in crystallization of the respective compounds, which were washed with additional ether. According to this procedure compounds **98–109** were prepared.

Remark: Debenzylation of protected bis(1*H*-indol-2-yl)methanones bearing also a chloro substituent resulted in addition in cleavage of the C–Cl bond yielding the respective unhalogenated 5-hydroxy compounds.

(5-Hydroxy-1*H*-indol-2-yl)-(4-methyl-1*H*-indol-2-yl)methanone (98). Yield: 0.90 g (79%). Mp: dec >82 °C. Anal. (C₁₈H₁₄N₂O₂): C, H, N.

(5-Hydroxy-1*H*-indol-2-yl)-(5-methyl-1*H*-indol-2-yl)methanone (99). Yield: 0.21 g (24%). Mp: 225–226 °C. Anal. (C₁₈H₁₄N₂O₂·1/4 MeCO₂Et): C, H, N.

(5-Hydroxy-1*H*-indol-2-yl)-(6-methyl-1*H*-indol-2-yl)methanone (100). Yield: 0.21 g (63%). Mp: 273.3–273.5 °C. Anal. (C₁₈H₁₄N₂O₂): C, H, N.

(7-Ethyl-1*H*-indol-2-yl)-(5-hydroxy-1*H*-indol-2-yl)methanone (101). Yield: 0.25 g (54%). Mp: 197–199 °C. Anal. (C₁₉H₁₆N₂O₂·1/3 MeCO₂Et): C, H, N.

Bis-(5-hydroxy-1*H*-indol-2-yl)methanone (102). Yield: 0.11 g (21%). Mp: dec 215 °C. Anal. (C₁₇H₁₂N₂O₃·1/6 MeCO₂Et): C, H, N.

(5-Hydroxy-1*H*-indol-2-yl)-(4-methoxy-1*H*-indol-2-yl)methanone (103). Yield: 0.62 g (48%). Mp: 251–252 °C. Anal. (C₁₈H₁₄N₂O₃): C, H, N.

(5-Hydroxy-1*H*-indol-2-yl)-(6-methoxy-1*H*-indol-2-yl)methanone (104). Yield: 1.95 g (92%). Mp: 165.1–169.4 °C. Anal. (C₁₈H₁₄N₂O₃): C, H, N.

(5-Hydroxy-1*H*-indol-2-yl)-(7-methoxy-1*H*-indol-2-yl)methanone (105). Yield: 0.54 g (29%). Mp: 252.2–253.5 °C. Anal. (C₁₈H₁₄N₂O₃): C, H, N.

(4-Fluoro-1*H*-indol-2-yl)-(5-hydroxy-1*H*-indol-2-yl)methanone (106). Yield: 0.08 g (52%). Mp: dec >270 °C. Anal. (C₁₇H₁₁FN₂O₂): C, H, N.

(5-Fluoro-1*H*-indol-2-yl)-(5-hydroxy-1*H*-indol-2-yl)methanone (107). Yield: 1.68 g (94%). Mp: 204.7–224.7 °C. Anal. (C₁₇H₁₁FN₂O₂): C, H, N.

(6-Fluoro-1*H*-indol-2-yl)-(5-hydroxy-1*H*-indol-2-yl)methanone (108). Yield: 0.19 g (55%). Mp: 261.4–262.2 °C. Anal. (C₁₇H₁₁FN₂O₂·1/2 EtOH): C, H, N.

(7-Fluoro-1*H*-indol-2-yl)-(5-hydroxy-1*H*-indol-2-yl)methanone (109). Yield: 0.67 g (73%). Mp: 262 °C. Anal. (C₁₇H₁₁FN₂O₂): C, H, N.

Procedure H for the Preparation of Alkyl Derivatives: Alkylation of (5-Hydroxy-1*H*-indol-2-yl)-(1*H*-indol-2-yl)methanones. The respective alkyl halide, respective of its hydrohalide (1.50 mmol), was added together with KOH (3.00 mmol) in the case of alkyl halide, in case of hydrohalides as alkylating agents 4.50 mmol) to a solution of **98**, **104**, or **107** (1.00 mmol) in acetone (40 mL). The mixture was stirred at room temperature for 15 min till 3 h (TLC control). The mixture was poured into ice–water (250 mL) and extracted with ethyl acetate. The organic layer was dried (Na₂SO₄) and the solvent removed in vacuo. The crude product was purified by column chromatography (SiO₂, ethyl acetate/methanol 1:1) and crystallized from ethyl acetate/diethyl ether to yield the compounds as yellow crystals. According to this procedure, compounds **112–115** were prepared.

[5-(2-Dimethylaminoethoxy)-1*H*-indol-2-yl]-(6-methoxy-1*H*-indol-2-yl)methanone (112). Yield: 0.09 g (24%). Mp: 189.4–192.5 °C. Anal. (C₂₂H₂₃N₃O₃·1/4 H₂O): C, H, N.

(4-Methyl-1*H*-indol-2-yl)-[5-(2-piperidin-1-yl-ethoxy)-1*H*-indol-2-yl]methanone (113). Yield: 0.08 g (23%). Mp: 172 °C. Anal. (C₂₅H₂₇N₃O₂): C, H, N.

(6-Methoxy-1*H*-indol-2-yl)-[5-(2-piperidin-1-yl-ethoxy)-1*H*-indol-2-yl]methanone (114). Yield: 0.08 g (19%). Mp: 161.5–163.2 °C. Anal. (C₂₅H₂₇N₃O₃·1/2 H₂O): C, H, N.

(5-Fluoro-1*H*-indol-2-yl)-[5-(2-piperidin-1-yl-ethoxy)-1*H*-indol-2-yl]methanone (115). Yield: 0.11 g (27%). Mp: 147.9–148.9 °C. Anal. (C₂₄H₂₄FN₃O₂): C, H, N.

Procedure I: Simultaneous Phenylsulfonyl and tert-Butyldimethylsilyl Deprotection of 69 and 70 with NaOH. The N-protected halo derivative (1.56 mmol) and 50 mL of a 10% aq. NaOH solution were stirred at 60 °C for 8 to 12 h under nitrogen atmosphere. After completion of the reaction (TLC control), the mixture was neutralized with aq. HCl, filtered, and dried. The crude product was purified by column chromatography (SiO₂, DCM).

(4-Chloro-1*H*-indol-2-yl)-(5-hydroxy-1*H*-indol-2-yl)methanone (110). Yield: 0.17 g (26%). Mp: 262 °C. Anal. (C₁₇H₁₁-ClN₂O₂): C, H, N.

(4-Bromo-1*H*-indol-2-yl)-(5-hydroxy-1*H*-indol-2-yl)methanone (111). Yield: 0.04 g (22%). Mp: 207–210 °C. Anal. (C₁₇H₁₁BrN₂O₂): C, H, N.

Procedure J: Preparation of Bisindolylmethanes. A suspension of the appropriate bisindolylmethanone derivative (5.0 mmol), KOH (25.0 mmol) and hydrazine hydrate (0.5 mL) in ethylene glycol was heated to 195 °C (200 W) within 1 h in a focused microwave apparatus (CEM Discover). A 50 mL amount of sat. ammonium chloride aq. solution was added to the mixture, which was then extracted with DCM. The combined organic extracts were dried over Na₂SO₄, the solvent was removed under vacuo, and the crude product was subjected to chromatography (SiO₂, DCM).

(1*H*-Indol-2-yl)-(5-methoxy-1*H*-indol-2-yl)methane¹² (116). Preparation from (1*H*-indol-2-yl)-(5-methoxy-1*H*-indol-2-yl)-methanone **4b**. Yield: 0.28 g (84%). Mp: 112 °C.

(5-Fluoro-1*H*-indol-2-yl)-(5-methoxy-1*H*-indol-2-yl)-methane (117). Preparation from (5-fluoro-1*H*-indol-2-yl)-(5-methoxy-1*H*-indol-2-yl)-methanone **78**. Yield: 0.15 g (60%). Mp: 130.2–130.3 °C. Anal. (C₁₈H₁₅FN₂O): C, H, N.

Biochemical and Cellular Assays. Most cell lines, antibodies, and cDNAs used in this study were described earlier.^{11–13} A GST-Abl construct³⁸ was kindly provided by Dr. B. Druker (Oregon University). K562 cells were obtained from the German Collection of Cells and Microorganisms (Braunschweig). Anti-Abl antibodies (cat. # 2862) and anti-active Abl antibodies (cat. # 2861) were from Cell Signaling (Frankfurt, Germany).

Assays for FLT3 and PDGFR- β autophosphorylation in transiently transfected HEK293 cells and for PDGFR autophosphorylation in Swiss3T3 cells have also been previously described.^{11,12} For measuring autophosphorylation of endogenous FLT3 in EOL-1 cells, 5 \times 10⁶ cells per well were seeded into 12-well plates with RPMI1640 medium without serum. Inhibitors were added from 100-fold concentrated stocks directly into the medium (final DMSO concentration 1%), and plates were incubated at 37 °C, 5% CO₂ for 1 h. Stimulation was carried out with FL (50 ng/mL or solvent for control) at room temperature for 10 min. Cells were transferred to ice and lysed in 1 mL of TX100-containing lysis buffer.¹¹ Cell extracts were subjected to incubation with 15 μ L (1:1 slurry) of wheat germ agglutinin-agarose (Amersham) with end-over-end rotation at 4 °C for 1 h. The beads were washed twice with lysis buffer and extracted with SDS–PAGE sample buffer at 50 °C for 20 min. Immunoblotting and determination of IC₅₀ values were performed as described.¹²

To measure FLT3-dependent cell proliferation, 32Dcl3 cells stably transfected with hFLT3-ITD, or wild-type FLT3, kindly provided by C. Choudhary and H. Serve (University of Münster)³⁹ were employed. Proliferation assays were performed as described earlier.¹³ In brief, 10⁵ cells per well were seeded in 96-well plates in RPMI1640 medium, supplemented with 10% FCS. IL-3 (3 ng/mL R&D Systems) was added as indicated in the corresponding figure legend. Inhibitors or solvent DMSO were added (final DMSO concentration 0.1%), and cells were cultivated for 2 or 3 days. At this time-point, cell amounts were determined using 3-(4,5-dimethylthiazol-2-yl)-2,5-diphenyl-3*H*-tetrazol-2-ium bromide (MTT) with a kit of Roche (Mannheim) according to the instructions of the manufacturer. The effect of compounds on KIT-dependent cell proliferation was assayed exactly as described before.²³

For in vitro kinase assays, GST-fusion proteins containing the cytoplasmic domains of wild-type FLT3, or human PDGFR- β , were obtained as described earlier.^{12,13} As exogenous substrate, a synthetic peptide corresponding to the PDGFR- β autophosphorylation site tyrosine 751 with the sequence KKKSKDESVDYVPMLDMKG was employed. Approximately 100 ng of recombinant kinase were incubated with inhibitors (6 concentrations) or DMSO (solvent, final concentration 1%) on ice in a reaction mixture containing 50 mM Hepes, pH 7.5, 5 mM MnCl₂, 0.1 mM sodium orthovanadate, and 2 mM substrate peptide in a total volume of 95 μ L for 15 min. Then, [32P] γ ATP was added (5 μ L, 2–5 μ Ci), and the reaction

mixture was incubated at 30 °C for 20 min. A 20 μ L aliquot was taken before the start and at the end of the incubation. Aliquots were mixed with 20 μ L of 500 mM EDTA, pH 8.0, 2 mg/mL bovine serum albumin. Protein was precipitated by addition of 20 μ L of 20% (w/w) ice-cold trichloroacetic acid, incubation on ice for 30 min, and centrifugation in a microfuge for 5 min. Two 20 μ L aliquots of the supernatant were spotted onto phosphocellulose (Whatman P81). After drying, the membrane was washed with 75 mM phosphoric acid four times for at least 5 min, dried again, and exposed to an imaging screen of a BioRad GS250 molecular imager. Relative incorporation of radioactivity, corrected by subtraction of the values at the starting point, was used for calculation of IC₅₀ values. GST-FLT3 and GST-PDGFR- β had similar activity with this substrate peptide, and the reaction was nearly linear over at least 30 min.

Measurement of GST-Abl kinase activity in vitro was performed similar to that described by Corbin et al.³⁸ In brief, 0.5 μ g of a GST-fusion protein of the c-Abl catalytic domain was incubated in kinase buffer containing 50 mM Tris-HCl, pH 7.5, 10 mM MgCl₂, 10 μ M sodium orthovanadate, 1 mM dithiothreitol, and inhibitor or solvent control (added from a 100-fold stock solution in DMSO) on ice for 10 min. Then, ATP was added (1 μ Ci [32P] γ -ATP, final ATP concentration 111 nM, final volume 30 μ L), and samples were incubated at 30 °C for 30 min with agitation (500 rpm). The reaction was quenched by addition of 10 μ L of 6-fold concentrated SDS–PAGE sample buffer. Samples were subjected to electrophoresis, and gels were stained with Coomassie and dried. Radioactivity incorporated into the GST-Abl protein was quantified using a BioRad GS250 molecular imager and normalized to fusion protein amount in the sample revealed by Coomassie-staining and densitometric scanning. Inhibition of autophosphorylation of Bcr-Abl in K562 cells was analyzed by incubating 2 \times 10⁶ cells in 1 mL of serum-free RPMI1640 medium with inhibitor or solvent control (1% DMSO) at 37 °C in a CO₂ incubator for 2 h. Cells were transferred into 1.5 mL tubes, spun down at 200g for 5 min, and lysed in 100 μ L of lysis buffer. Lysates were analyzed by SDS–PAGE in 7.5% gels, wet transferred to PVDF membranes, and immunodetected with anti-pAbl and anti-Abl antibodies.

All IC₅₀ values are derived from duplicate or triplicate determinations and were determined from a concentration curve comprising six concentrations using the program SigmaPlot (Systat Software Inc.) as described earlier.¹² The standard errors of the mean (SEM) are always in the range of \pm 50%.

Primary AML-cells were obtained from blood of patients with newly diagnosed acute myeloid leukaemia. Mononuclear cells (MNC) were isolated by means of Ficoll-Hypaque (Seromed, Berlin, Germany) density gradient centrifugation. The cells were incubated in medium supplemented with fetal calf serum for 24 h at 37 °C. Then, 200 000 cells were plated in 2 mL of medium with or without the kinase inhibitors. The incubation period was 96 h. Thereafter, cell cycle analysis was performed as previously described,⁴⁰ and the sub-G1 population was quantified. The spontaneous apoptosis rate in the individual patients ranged from 4.7 to 54.4%.

Molecular Modeling. An initial computer model of the FLT3 kinase was generated from the PDB crystal structure 1rjb¹⁴ using the molecular modeling package SYBYL 6.9 (Tripos Inc., St. Louis, MO) on a Silicon Graphics Octane workstation. After adding hydrogens, compound **98** was docked in different poses derived from previous results (ref 12 and references therein). The two possible binding conformations of **98**, sp/ap and sp/sp, their energies and rotational barriers were calculated by the semiempirical quantum chemical program AMPAC 6.55 (Semicem Inc., 7128 Summit, Shawnee, KS 66216) with the AM1 Hamiltonian, the TRUSTE minimization algorithm, and the COSMO water solvation model⁴¹ as implied in SYBYL 6.9. After docking, the FLT3-ligand complexes were energy minimized using the AMBER 4.1 force field⁴² with AMBER 95 charges for the protein (distance-dependent dielectricity constant 4, first 50 cycles with constrained backbone and the steepest descent method). For that purpose, compound **98** and other derivatives were provided with AMBER 4.1 atom types by analogy with corresponding amino acid atoms, as well as with

Gasteiger-Hueckel charges. New parameters describing the central NHC(CH)COC(CH)NH moiety had to be added to the AMBER 4.1 force field (derived from the Tripos force field and from comparison with similar AMBER parameters). The final minimization up to a RMS gradient of 0.05 kcal/(mol·Å) was performed with the Powell conjugate gradient method. Considerations on the PDGFR kinase were based on the FLT3 crystal structure with simple mutation of the only different binding site residue, FLT3 Phe-691, into PDGFR Thr-681. Handling of compound **82** and its docking into the PDGFR model were performed like that in the case of the FLT3—compound **98** complex.

Acknowledgment. This work was supported by a grant from the Deutsche Krebshilfe (10-2100-Do2, to F.D.B., S.D., and S.M.) and the Deutsche Krebshilfe grant Oncogene Networks in the Pathogenesis of AML (to F.D.B., T.F., and C.S.). We gratefully acknowledge provision of reagents from H. Serve (University of Münster) and B. Druker (University of Oregon), and thank Ulla Bergholz for excellent technical assistance.

Supporting Information Available: Spectroscopic data (IR, NMR, MS) and detailed combustion analyses. This material is available free of charge via the Internet at <http://pubs.acs.org>.

References

- Hanahan, D.; Weinberg, R. A. The hallmarks of cancer. *Cell* **2000**, *100*, 57–70.
- Blume-Jensen, P.; Hunter, T. Oncogenic kinase signalling. *Nature* **2001**, *411*, 355–365.
- Pietras, K.; Sjoblom, T.; Rubin, K.; Heldin, C. H.; Ostman, A. PDGFR receptors as cancer drug targets. *Cancer Cell* **2003**, *3*, 439–443.
- George, P.; Bali, P.; Cohen, P.; Tao, J.; Guo, F.; Sigua, C.; Vishvanath, A.; Fiskus, W.; Scuto, A.; Annavarapu, S.; Moscinski, L.; Bhalla, K. Cotreatment with 17-allylamino-demethoxygeldanamycin and FLT-3 kinase inhibitor PKC412 is highly effective against human acute myelogenous leukemia cells with mutant FLT-3. *Cancer Res.* **2004**, *64*, 3645–3652.
- Wilhelm, S. M.; Carter, C.; Tang, L.; Wilkie, D.; McNabola, A.; Rong, H.; Chen, C.; Zhang, X.; Vincent, P.; McHugh, M.; Cao, Y.; Shujath, J.; Gawlak, S.; Eveleigh, D.; Rowley, B.; Liu, L.; Adnane, L.; Lynch, M.; Auclair, D.; Taylor, I.; Gedrich, R.; Voznesensky, A.; Riedl, B.; Post, L. E.; Bollag, G.; Trail, P. A. BAY 43–9006 exhibits broad spectrum oral antitumor activity and targets the RAF/MEK/ERK pathway and receptor tyrosine kinases involved in tumor progression and angiogenesis. *Cancer Res.* **2004**, *64*, 7099–7109.
- Daub, H.; Specht, K.; Ullrich, A. Strategies to overcome resistance to targeted protein kinase inhibitors. *Nat. Rev. Drug. Discovery* **2004**, *3*, 1001–1010.
- Schmidt-Arras, D.; Schwable, J.; Bohmer, F. D.; Serve, H. Flt3 receptor tyrosine kinase as a drug target in leukemia. *Curr. Pharm. Des.* **2004**, *10*, 1867–1883.
- Ozeki, K.; Kiyoi, H.; Hirose, Y.; Iwai, M.; Ninomiya, M.; Kodera, Y.; Miyawaki, S.; Kuriyama, K.; Shimazaki, C.; Akiyama, H.; Nishimura, M.; Motoji, T.; Shinagawa, K.; Takeshita, A.; Ueda, R.; Ohno, R.; Emi, N.; Naoe, T. Biologic and clinical significance of the FLT3 transcript level in acute myeloid leukemia. *Blood* **2004**, *103*, 1901–1908.
- Komeno, Y.; Kurokawa, M.; Imai, Y.; Takeshita, M.; Matsumura, T.; Kubo, K.; Yoshino, T.; Nishiyama, U.; Kuwaki, T.; Kubo, K.; Osawa, T.; Ogawa, S.; Chiba, S.; Miwa, A.; Hirai, H. Identification of Ki23819, a highly potent inhibitor of kinase activity of mutant FLT3 receptor tyrosine kinase. *Leukemia* **2005**, *19*, 930–935.
- Sattler, M.; Verma, S.; Byrne, C. H.; Shrikhande, G.; Winkler, T.; Algate, P. A.; Rohrschneider, L. R.; Griffin, J. D. BCR/ABL directly inhibits expression of SHIP, an SH2-containing polyinositol-5-phosphatase involved in the regulation of hematopoiesis. *Mol. Cell. Biol.* **1999**, *19*, 7473–7480.
- Böhmer, F. D.; Karagoyozov, L.; Uecker, A.; Serve, H.; Botzki, A.; Mahboobi, S.; Dove, S. A single amino acid exchange inverts susceptibility of related receptor tyrosine kinases for the ATP site inhibitor STI-571. *J. Biol. Chem.* **2003**, *278*, 5148–5155.
- Mahboobi, S.; Teller, S.; Pongratz, H.; Hufsky, H.; Sellmer, A.; Botzki, A.; Uecker, A.; Beckers, T.; Baasner, S.; Schachtele, C.; Uberall, F.; Kassack, M. U.; Dove, S.; Böhmer, F.-D. Bis(1*H*-2-indolyl)methanones as a Novel Class of Inhibitors of the Platelet-Derived Growth Factor Receptor Kinase. *J. Med. Chem.* **2002**, *45*, 1002–1018.
- Teller, S.; Krämer, D.; Böhmer, S.-A.; F.Tse, K.; Small, D.; Mahboobi, S.; Wallrapp, C.; Beckers, T.; Kratz-Albers, K.; Schwable, J.; Serve, H.; Böhmer, F. D. Bis(1*H*-2-indolyl)-1-methanones as inhibitors of the hematopoietic tyrosine kinase Flt3. *Leukemia* **2002**, *16*, 1528–1534.
- Griffith, J.; Black, J.; Faerman, C.; Swenson, L.; Wynn, M.; Lu, F.; Lippke, J.; Saxena, K. The structural basis for autoinhibition of FLT3 by the juxtamembrane domain. *Mol. Cell.* **2004**, *13*, 169–178.
- Bentley, J. M.; Hebeisen, P.; Muller, M.; Richter, H.; Roever, S.; Mattei, P.; Taylor, S. Piperazine derivatives. WO 02/10169 A1 2002.
- Huang-Minlon A simple modification of the Wolff–Kishner Reduction. *J. Am. Chem. Soc.* **1946**, *68*, 2487–2488.
- Kovalenko, M.; Gazit, A.; Böhmer, A.; Rorsman, C.; Ronnstrand, L.; Heldin, C. H.; Waltenberger, J.; Böhmer, F. D.; Levitzki, A. Selective platelet-derived growth factor receptor kinase blockers reverse sis-transformation. *Cancer Res.* **1994**, *54*, 6106–6114.
- Tse, K. F.; Novelli, E.; Civin, C. I.; Bohmer, F. D.; Small, D. Inhibition of FLT3-mediated transformation by use of a tyrosine kinase inhibitor. *Leukemia* **2001**, *15*, 1001–1010.
- Mohammadi, M.; Froum, S.; Hamby, J. M.; Schroeder, M. C.; Panek, R. L.; Lu, G. H.; Eliseenkova, A. V.; Green, D.; Schlessinger, J.; Hubbard, S. R. Crystal structure of an angiogenesis inhibitor bound to the FGF receptor tyrosine kinase domain. *EMBO J.* **1998**, *17*, 5896–5904.
- Böhmer, F. D.; Karagoyozov, L.; Uecker, A.; Serve, H.; Botzki, A.; Mahboobi, S.; Dove, S. A Single Amino Acid Exchange Inverts Susceptibility of Related Receptor Tyrosine Kinase for the ATP Site Inhibitor STI-571. *J. Biol. Chem.* **2003**, *278*, 5148–5155.
- Nagar, B.; Bornmann, W. G.; Pellicana, P.; Schindler, T.; Veach, D. R.; Miller, W. T.; Clarkson, B.; Kuriyan, J. Crystal structure of the kinase domain of c-Abl in complex with the small molecule inhibitors PD173955 and imatinib (STI-571). *Cancer Res.* **2002**, *62*, 4236–4243.
- Weisberg, E.; Boulton, C.; Kelly, L. M.; Manley, P.; Fabbro, D.; Meyer, T.; Gilliland, D. G.; Griffin, J. D. Inhibition of mutant FLT3 receptors in leukemia cells by the small molecule tyrosine kinase inhibitor PKC412. *Cancer Cell* **2002**, *1*, 433–443.
- Cammenga, J.; Horn, S.; Bergholz, U.; Sommer, G.; Besmer, P.; Fiedler, W.; Stocking, C. Extracellular KIT receptor mutants, commonly found in core binding factor AML, are constitutively active and respond to imatinib mesylate. *Blood* **2005**, *106*, 3958–3961.
- Moasser, M. M.; Srethapakdi, M.; Sachar, K. S.; Kraker, A. J.; Rosen, N. Inhibition of Src kinases by a selective tyrosine kinase inhibitor causes mitotic arrest. *Cancer Res.* **1999**, *59*, 6145–6152.
- Sundberg, R. J.; Russel, F. Syntheses with N-Protected 2-Lithioindoles. *J. Org. Chem.* **1973**, *38*, 3324–3330.
- Ishibashi, H.; Akamatsu, S.; Iriyama, H.; Ikeda, M. Convenient synthesis of 4-alkyl, alkenyl, and alkynyl substituted N-(phenylsulfonyl)indoles. *Chem. Pharm. Bull.* **1994**, *42*, 2150–2153.
- Mahboobi, S.; Pongratz, H.; Hufsky, H.; Hockemeyer, J.; Frieser, M.; Lyssenko, A.; Paper, D. H.; Bürgermeister, J.; Böhmer, F.-D.; Fiebig, H.-H.; Burger, A. M.; Baasner, S.; Beckers, T. Synthetic 2-Aroylindole Derivatives as a New Class of Potent Tubulin-Inhibitory, Antimitotic Agents. *J. Med. Chem.* **2001**, *44*, 4535–4553.
- Wenkert, E.; Moeller, P. D. R.; Pietre, S. R. Five-Membered Aromatic Heterocycles as Dienophile in Diels–Alder Reactions. Furan, Pyrrole and Indole. *J. Am. Chem. Soc.* **1988**, *110*, 7188–7194.
- Ishibashi, H.; Akamatsu, S.; Iriyama, H.; Hanaoka, K.; Tabata, T.; Ikeda, M. New, concise route to indoles bearing oxygen or sulfur substituent at the 4-position. Synthesis of (±)- and (S)-(-)-pindolol and (±)-chuangxinmycin. *Chem. Pharm. Bull.* **1994**, *42*, 271–276.
- Sundberg, R. J.; Parton, R. L. Lithiation of Methoxyindoles. *J. Org. Chem.* **1976**, *41*, 163–165.
- Fuji, M.; Muratake, H.; Natsume, M. Preparation of alkyl-substituted indoles in the benzene portion. Part 6. Synthetic procedure for 4-, 5-, 6- or 7-alkoxy- and hydroxyindole derivatives. *Chem. Pharm. Bull.* **1992**, *40*, 2344–2352.
- Matsumoto, M.; Ishida, Y.; Hatanaka, N. A facile one-step synthesis of 4-aminoindoles from 5-halo-4-oxo-4,5,6,7-tetrahydroindoles. *Heterocycles* **1986**, *24*, 1667–1674.
- Ketcha, D. M.; Gribble, G. W. A convenient synthesis of 3-acylindoles via Friedel Crafts acylation of 1-(phenylsulfonyl)indole. A new route to pyridocarbazole-5, 11-quinones and ellipticine. *J. Org. Chem.* **1985**, *50*, 5451–5457.
- Kano, S.; Sugino, E.; Shibuya, S.; Hibino, S. Synthesis of Carbazole Alkaloids Hyellazole and 6-Chlorohyellazole. *J. Org. Chem.* **1981**, *46*, 3856–3859.
- Silvestri, R.; Martino, G. D.; Regina, G. L.; Artico, M.; Massa, S.; Vargiu, L.; Mura, M.; Loi, A. G.; Marceddu, T.; Colla, P. L. Novel Indolyl Aryl Sulfones Active against HIV-1 Carrying NNRTI Resistance Mutations: Synthesis and SAR Studies. *J. Med. Chem.* **2003**, *46*, 248–2493.

- (36) Ketcha, D. M. The manganese(III) acetate oxidation of N-protected indolines. *Tetrahedron Lett.* **1988**, *29*, 2151–2154.
- (37) Saulnier, M. G.; Gribble, G. W. Generation and Reactions of 3-Lithio-1-(phenylsulfonyl)indole. *J. Org. Chem.* **1982**, *47*, 757–761.
- (38) Corbin, A. S.; Buchdunger, E.; Pascal, F.; Druker, B. J. Analysis of the structural basis of specificity of inhibition of the Abl kinase by ST1571. *J. Biol. Chem.* **2002**, *277*, 32214–32219.
- (39) Mizuki, M.; Schwable, J.; Steur, C.; Choudhary, C.; Agrawal, S.; Sargin, B.; Steffen, B.; Matsumura, I.; Kanakura, Y.; Bohmer, F. D.; Muller-Tidow, C.; Berdel, W. E.; Serve, H. Suppression of myeloid transcription factors and induction of STAT response genes by AML-specific Flt3 mutations. *Blood* **2003**, *101*, 3164–3173.
- (40) Kindler, T.; Breitenbuecher, F.; Kasper, S.; Stevens, T.; Carius, B.; Gschaidmeier, H.; Huber, C.; Fischer, T. In BCR-ABL-positive cells, STAT-5 tyrosine-phosphorylation integrates signals induced by imatinib mesylate and Ara-C. *Leukemia* **2003**, *17*, 999–1009.
- (41) Klamt, A. Conductor-like Screening Model for Real Solvents: A New Approach to the Quantitative Calculation of Solvation Phenomena. *J. Phys. Chem.* **1995**, *99*, 2224–2235.
- (42) Cornell, W. D.; Cieplak, P.; Bayly, C. I.; Gould, I. R.; Merz, K. M. J.; Ferguson, D. M.; Spellmeyer, D. C.; Fox, T.; Caldwell, J. W.; Kollman, P. A. A second generation force field for the simulation of proteins and nucleic acids. *J. Am. Chem. Soc.* **1995**, *117*, 5179–5197.

JM058033I